CHAPTER 3B

Rhodium(III)-Catalyzed Dehydrogenative Annulation and Spirocyclization of 2-Arylindoles and 2-(1*H*-Pyrazol-1-yl)-1*H*-indoles with Maleimides: A Facile Access to Isogranulatimide Alkaloid Analogues

Chapter 3B

3.3B.1 INTRODUCTION

Transition metal-catalyzed C–H bond functionalization for the construction of carbon-carbon and carbon-heteroatom bonds is an efficient and straightforward protocol that has found applicability in various chemical transformations.[1-5] As a result, this strategy has been explosively explored in the organic synthesis and gained a huge impact to construct complex cyclic scaffolds from cheap and easily available raw materials. However, the selective C–H bond activation is a major concern, and by the utilization of directing group, it has been resolved to some extent.[6-8] Apart from its advantages in selective C–H bond functionalization, the removal of directing group from the substrate is the key challenge. In this regard, annulation strategy rapidly built up for the construction of hetero and carbocycles in recent years.[9-11] Transition metal-catalyzed C–H annulation and spirocyclization has gained considerable interest of chemists to synthesize carbocyclic and heterocyclic molecules in a rapid and sustainable manner to overcomes this disadvantages.[12-15] In addition, heteroatom is used as a directing group in the annulation reaction to avoid the removal of directing group after synthetic transformations. Because its strong coordination with metal followed by cyclometallation at the adjacent position and subsequent C–H functionalization/annulation with various partners made the protocol more ideal.[16] Among various transition metal catalysts, Rh(III)-catalyzed annulation reactions particularly attracted more attention.[17-18] The operational simplicity, selectivity, and wide functional group tolerance are the significant features to make this strategy more ideal and sustainable.

Maleimides are the key core moiety exclusively found in many natural products and pharmaceuticals with various biological activities **(Figure 3.3B.1)**.[19] Moreover, maleimides can be easily transformed into biologically potent pyrrolidines, succinimides, and γ-lactams.[20-22] In addition, it has been used as the two-carbon electrophilic coupling partner in several organic transformations such as C–H activation, annulation, and spirocyclization reactions with the metal catalyst.[23] With the recent advancement, Rh(III)-catalyzed annulation and spirocyclization of several dipolarophile substrates with maleimides have been developed.[24-25] In 2019, Jeganmohan *et al*. reported the Rh(III)-catalyzed synthesis of isoindolinone spirosuccinimides **(4)** by monodentate amide ligand assisted 1,1-cyclization of *N*-methoxy benzamides **(1)** with maleimides **(2)** *via* C–H/N–H/O–H bond activation **(Scheme 3.3B.1a)**.[26] The reaction was performed in a redox-free manner by utilization of internal oxidant. The wide functional group tolerance and no need of external oxidants are the key features of the protocol. The detailed mechanistic study has

been described with the help of isolation of metallocycle intermediate, deuterium labelling experiment, and DFT studies. It revealed that the internally generated AcOH is responsible for the cleavage of N-OMe bond and oxidation of Rh(I) to Rh(III) species. Similarly, Kim and co-workers developed synthesis of bioactive spiroisoindolinone derivatives **(4)** *via* Rh(III)-catalyzed [3 + 2] annulation of *N*-acyl ketimines generated *in-situ* from 3-hydroxyisoindolinones **(3)** with maleimides **(2) (Scheme 3.3B.1b)**.[27] The other activated olefins like acrylates, maleates, fumarates, cinnamates, and quinones also effectively participated in the reaction to afford the spiroannulated products in good to excellent yields.

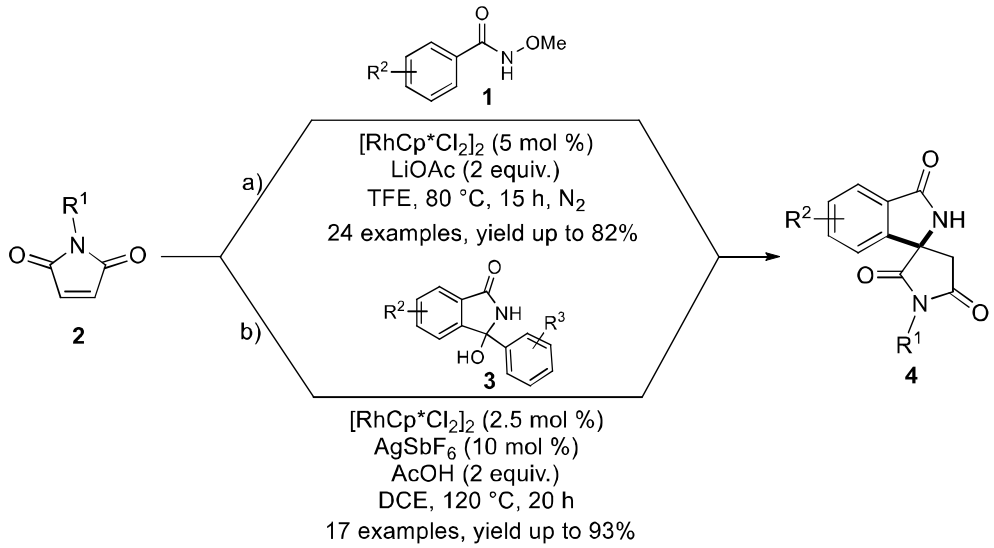

Scheme 3.3B.1 Rh(III)-catalyzed synthesis of isoindolinone spirosuccinimides.

Kim and team described the synthesis of pharmacologically privileged 1-aminoindane derivatives **(6)** using Rh(III)-catalyzed cross-coupling of *N*-sulfonyl aldimines **(5)** with maleimides **(2) (Scheme 3.3B.2)**.[25] The other olefins also reacted efficiently to access the 1-aminoindane derivatives with excellent diastereoselectivity and good functional group compatibility.

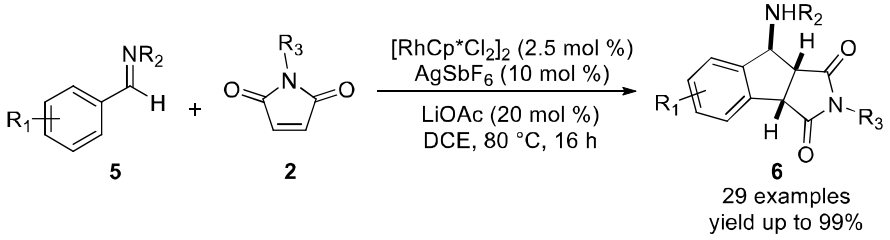

Scheme 3.3B.2 Rh(III)-catalyzed cross-coupling of *N*-sulfonyl aldimines with maleimides.

Fan and co-workers demonstrated the Rh(III)-catalyzed condition dependent dehydrogenative annulation of 2-arylindazoles **(7)** with maleimides **(2)** for the synthesis of indazolo[2,3-*a*]pyrrolo[3,4-*c*]quinolinones **(8)** or spiroindolo-[1,2-*b*]indazole-11,3′-pyrrolidinones **(9) (Scheme 3.3B.3)**.[28] The selectivity of the cyclic or spiro products has been achieved by switching the additives. The significant features exhibited readily available substrate and excellent atom economy with high regioselectivity.

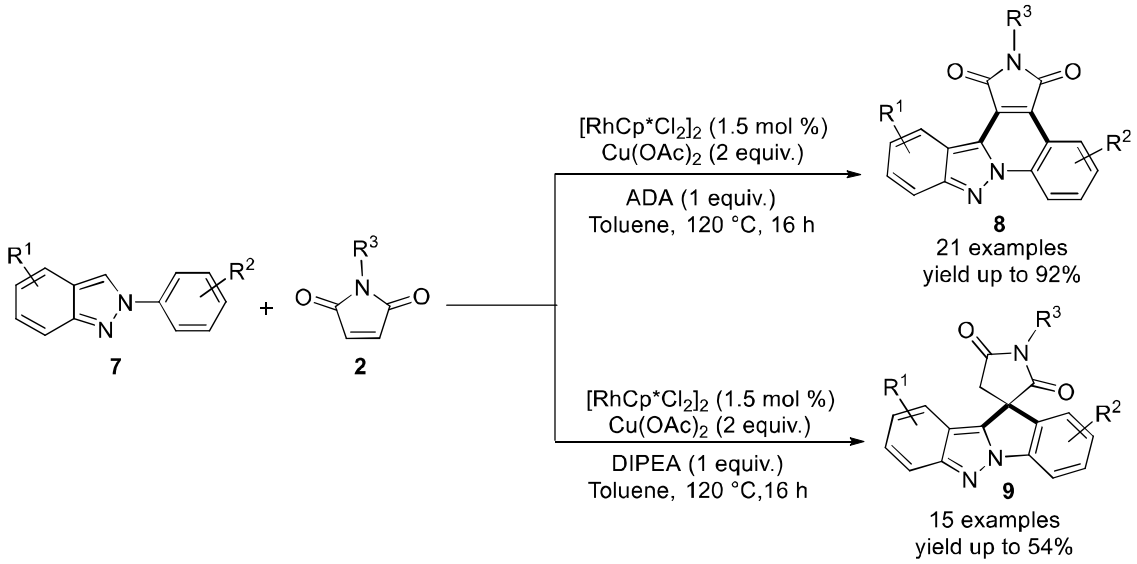

Scheme 3.3B.3 Rh(III)-catalyzed annulation of 2-arylindazoles with maleimides.

Bao group reported an effective method for the synthesis of pyrrolo[3,4-*b*]indole-1,3-diones **(11)** through Rh(III)-catalyzed C H activation and annulation of arylhydrazines **(10)** with maleimides **(2) (Scheme 3.3B.4)**.[29] The easily available raw materials, mild reaction condition, compatibility of functional groups, and experimental simplicity make this protocol more attractive towards the synthesis of fused heterocycles.

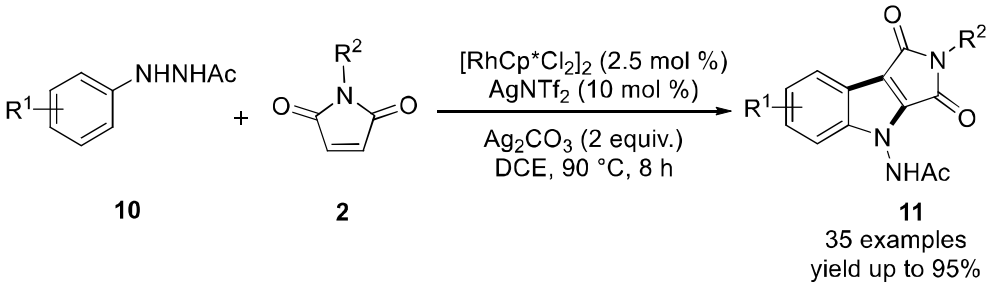

Scheme 3.3B.4 Rh(III)-catalyzed annulation of arylhydrazines with maleimides.

In 2019, Lee and groups developed a novel and facile Rh(III)-catalyzed approach to afford the biologically interesting spiro-fused pyrrolidinedione heterocycles **(13)** *via* cascade C–H activation and spirocyclization of 2-arylquinazolin-4(3*H*)-ones **(12)** with maleimides **(2) (Scheme 3.3B.5)**.[30] The sequential *ortho* C–H functionalization and spirocyclization followed by aza-Michael addition to formed C–C and C–N bond in single-step process were the main steps of the protocol. The notable features consist of one-step synthesis, broad substrate scope, high atom economy, regioselectivity, and wide functional group tolerance.

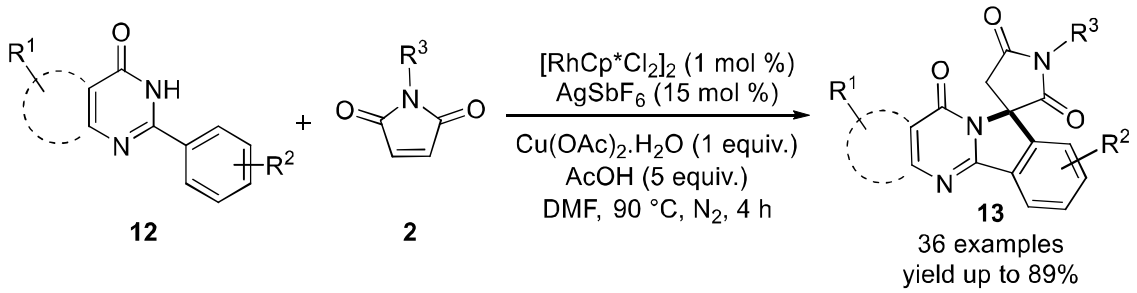

Scheme 3.3B.5 Rh(III)-catalyzed spirocyclization of 2-arylquinazolin-4(3*H*)-ones with maleimides.

On the other hand, indole is the privileged class of the heterocyclic molecules found in various natural products, pharmaceuticals, and synthetic drugs.[31-33] Importantly, a large number of alkaloids contain the indole attached maleimide units, such as granulatimide and isogranulatimide and these natural alkaloids isolated from the ascidian *Didemnum granulatum* **(Figure 3.3B.1)**.[34-35] Therefore, rhodium,[36] ruthenium,[37] cobalt,[38-40] and manganese[41] catalysts have been widely explored for the synthesis of 3-(indolyl)succinimides by coupling of indoles with maleimides. Although the existing methods are usually effective and reliable, but still the coupling between 2-arylindoles with maleimides is less explored.[42]

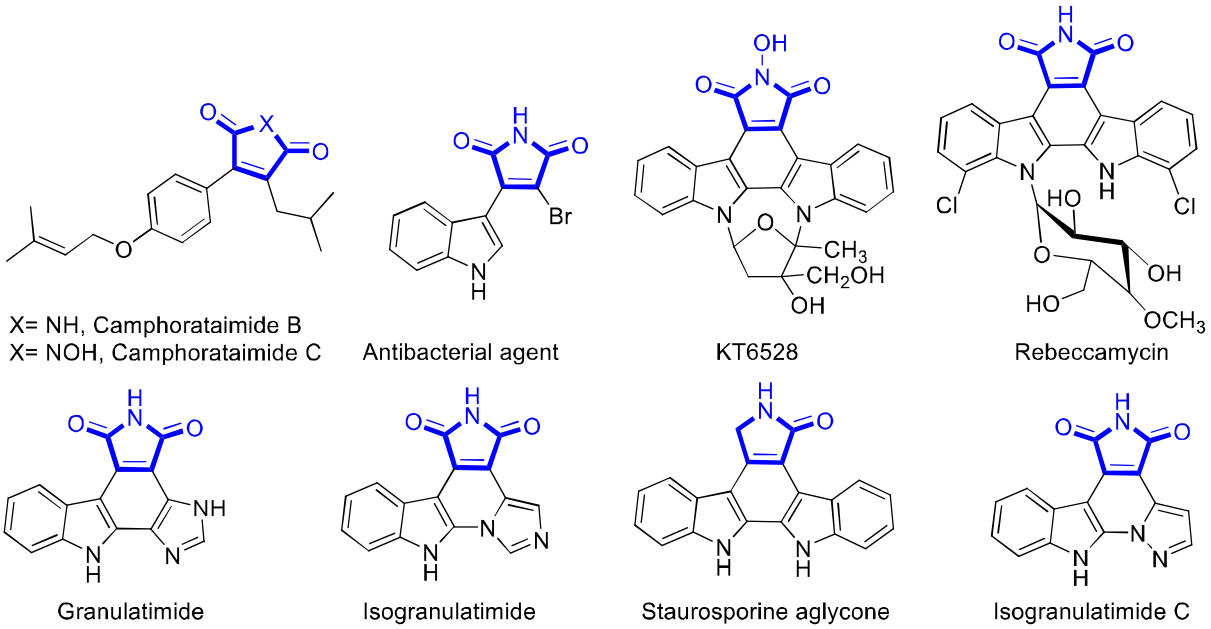

Figure 3.3B.1 Maleimide containing natural products and marine alkaloids

Fused carbazole is also an important class of indoles, which is found in several bioactive organic molecules, naturally occurring alkaloids, and organic electroluminescent materials.[43-45] Thus, numerous synthetic pathways have been reported towards the synthesis of fused carbazole.[46-48] In particular, Rh(III)-catalyzed annulation of 2-arylindoles with numerous coupling partners such as ketenes,[49] alkenes,[50-51] alkynes,[52-53] sulfoxonium ylides,[54] α-diazo carbonyl compounds,[55] and quinone monoacetals[56-57] have been exclusively demonstrated. In 2018, Li and co-workers reported Rh(III)-catalyzed oxidative [4 + 2] annulation of 2-arylindoles **(14)** with ketenes **(15)** for the synthesis of cyclic products **(Scheme 3.3B.6)**.[49] The cyclic products with quaternary stereogenic center **(16)** have been afforded by the utilization of highly reactive C3 position of 2-phenylindoles followed by reductive elimination process. In addition, high chemoselectivity with broad substrate scopes are the significant features of this method.

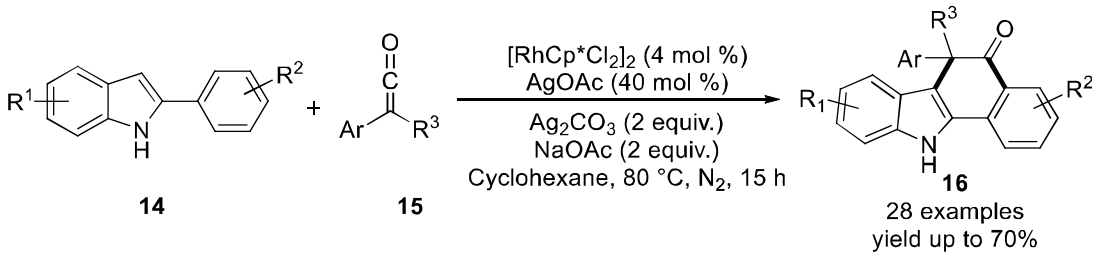

Scheme 3.3B.6 Rh(III)-catalyzed oxidative annulation of 2-arylindoles with ketenes.

Huang *et al*. reported solvent dependant Rh(III)-catalyzed *ortho* C–H olefination of 2-arylindoles **(14)** with substituted alkenes **(17)** to synthesize biologically important 6*H*-isoindolo[2,1-*a*]indole derivatives **(19) (Scheme 3.3B.7)**.[50] The *ortho* C–H olefination takes place by NH-indole-directed C–H bond activation and subsequent intramolecular aza-Michael reaction to afford the products in good to excellent yields. Interestingly, in ethyl acetate only *ortho*-alkenylated product **(18)** was isolated.

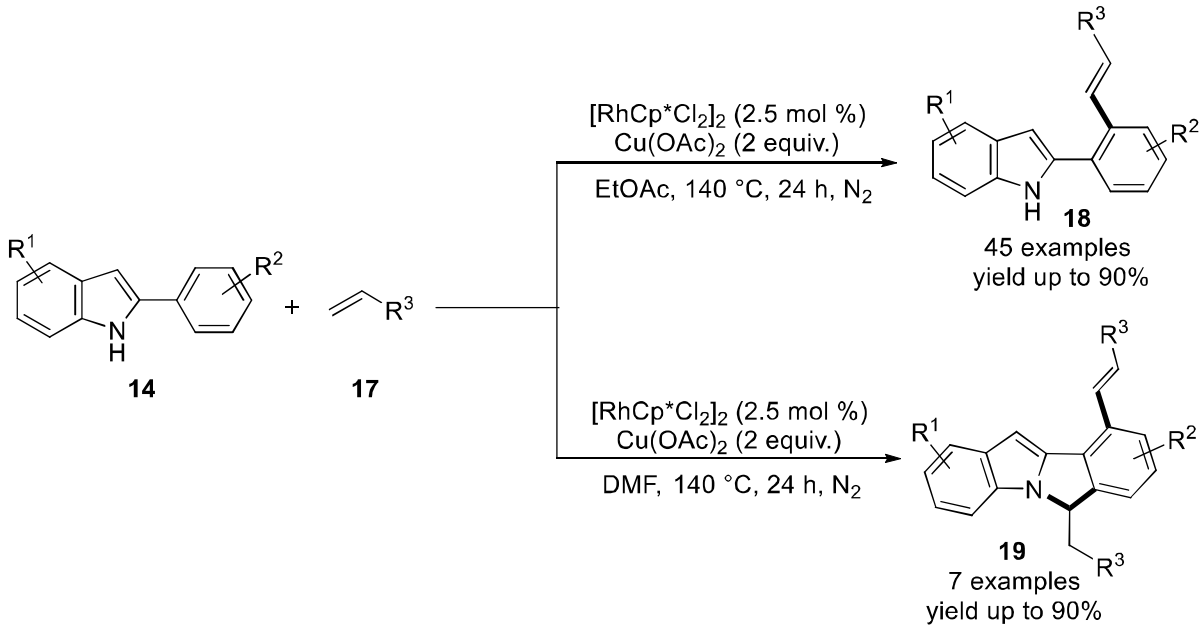

Scheme 3.3B.7 Rh(III)-catalyzed *ortho* olefination of 2-arylindoles with substituted alkenes.

Miura and group developed an efficient and straightforward protocol for the synthesis of indolo[2,1-*a*]isoquinoline derivatives **(21)** by using Rh(III)-catalyzed two-fold C–H activation of 2-arylindoles **(14)** with substituted alkynes **(20) (Scheme 3.3B.8)**.[52] Some of the annulated products exhibited solid-state fluorescence properties.

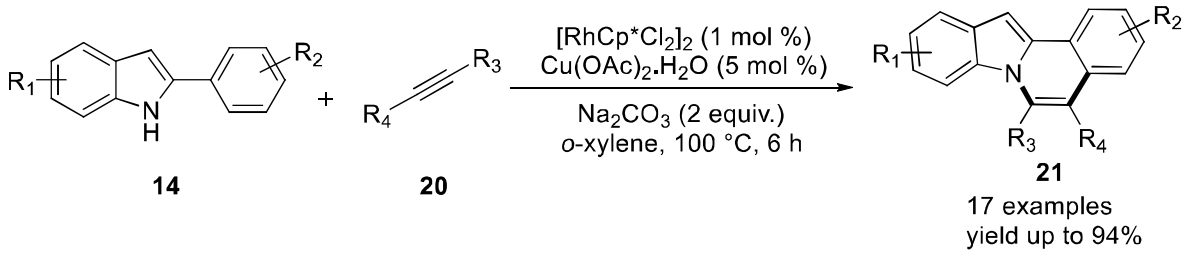

Scheme 3.3B.8 Rh(III)-catalyzed annulation of 2-arylindoles with alkynes.

In 2018, Fan *et al*. developed Rh(III)-catalyzed selective synthesis of benzo[*a*]carbazoles **(26)** and indolo[2,1-*a*]isoquinolines **(29)** through C–H alkylation followed by intramolecular condensation of the 2-arylindoles **(14)** with β-carbonyl sulfoxonium ylides **(22)** as stable carbene precursors and bifunctional C2 synthons **(Scheme 3.3B.9)**.[54] In addition, described method was equally applicable for 2-arylindole-3-carbaldehydes **(23)**, 2-arylindole-3-carbonitriles **(24)** or 2-aryl-3-methylindoles **(25)** with sulfoxonium ylides under optimum condition to the selective formation of 5-acylbenzo[*a*]carbazoles **(27)**, 6-amino-5-acylbenzo[*a*]carbazoles **(28)** or 12-methylindolo[2,1-*a*]isoquinolines **(29)**, respectively. The notable key points included an easily available substrate, broad substrate scope with high chem- and regioselectivity.

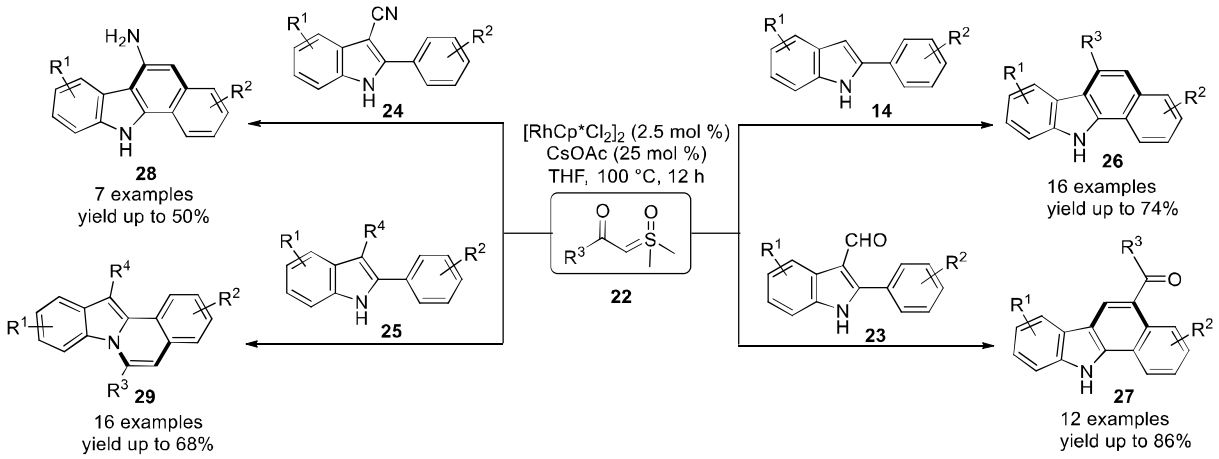

Scheme 3.3B.9 Rh(III)-catalyzed oxidative annulation of substituted 2-arylindoles with sulfoxonium ylides.

Further they reported an efficient synthetic approach for the synthesis of benzo[*a*]carbazoles **(31)** or 6-aminobenzo[*a*]carbazoles **(32)** using Rh(III)-catalyzed cascade reactions of 2-arylindoles **(14)** or 2-arylindole-3-carbonitriles **(24)** with α-diazo carbonyl compounds **(30) (Scheme 3.3B.10)**.[55] Remarkably, the readily available substrate, good functional group compatibility, high atom-efficiency, and regioselectivity are the advantages of this synthetic strategy.

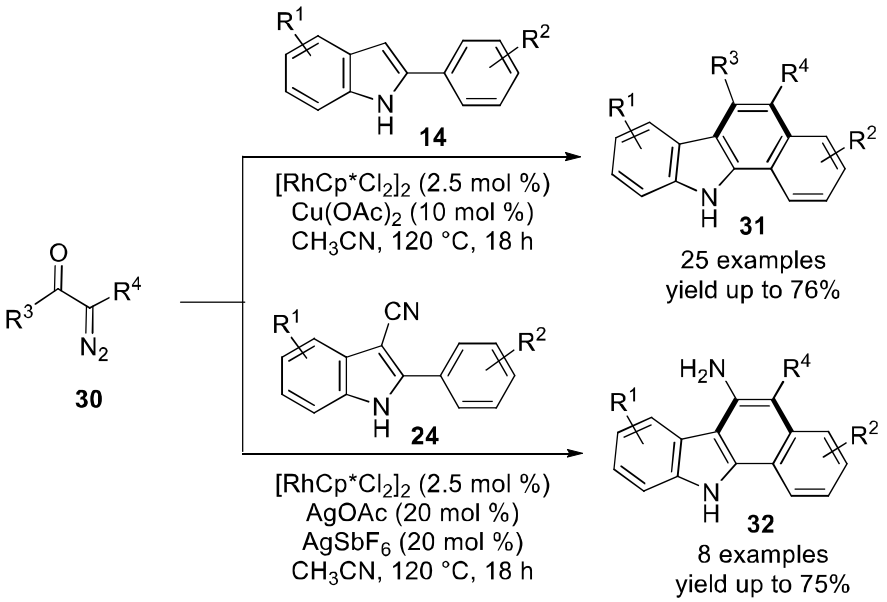

Scheme 3.3B.10 Rh(III)-catalyzed annulation of 2-arylindoles with α-diazo carbonyl compounds.

Li and co-workers reported the Rh(III)-catalyzed straightforward synthesis of [4,3,1]-bridged carbocycles **(34)** through two-fold C–H activation/formal Michael addition between 2-arylindoles **(14)** and quinone monoacetals **(33) (Scheme 3.3B.11)**.[57] Notably, exclusive C3 selectivity under redox-neutral condition and high atom and step economy are made this protocol more ideal and concise for the access of biologically relevant bridged cycles. Mechanistically, the deuterium labelling experiment revealed that C3 annulation takes place *via* dual C–H activation followed by a subsequent migratory insertion.

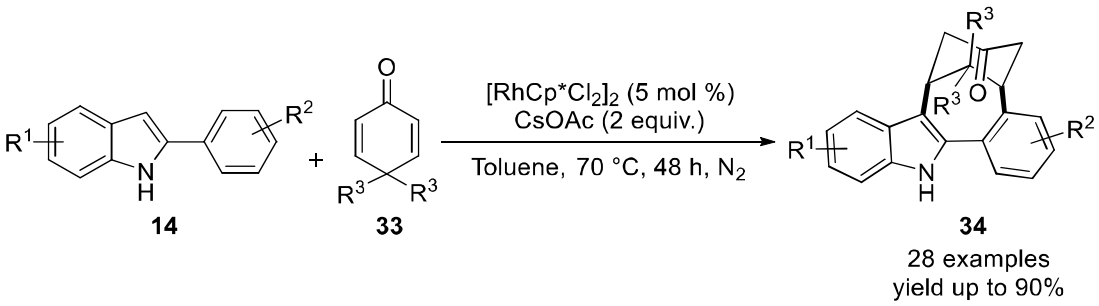

Scheme 3.3B.11 Rh(III)-catalyzed annulation of 2-arylindoles with quinone monoacetals.

Recently, Fan and group developed the substrate tunable Rh(III)-catalyzed oxidative annulation and spiroannulation of 2-arylindoles **(14)** with benzoquinone **(35)** afforded 9*H*-

dibenzo[*a*,*c*]carbazol-3-ols **(36)** and new spirocyclic products **(37) (Scheme 3.3B.12)**.[58] Interestingly, benzoquinone could act as a C2 synthon in case of substituted 2-arylindoles to furnish the dibenzo[*a*,*c*]carbazoles, whereas in the case of 3-substituted 2-arylindoles, benzoquinone switched to act as a C1 synthon to afford the spirocyclic products.

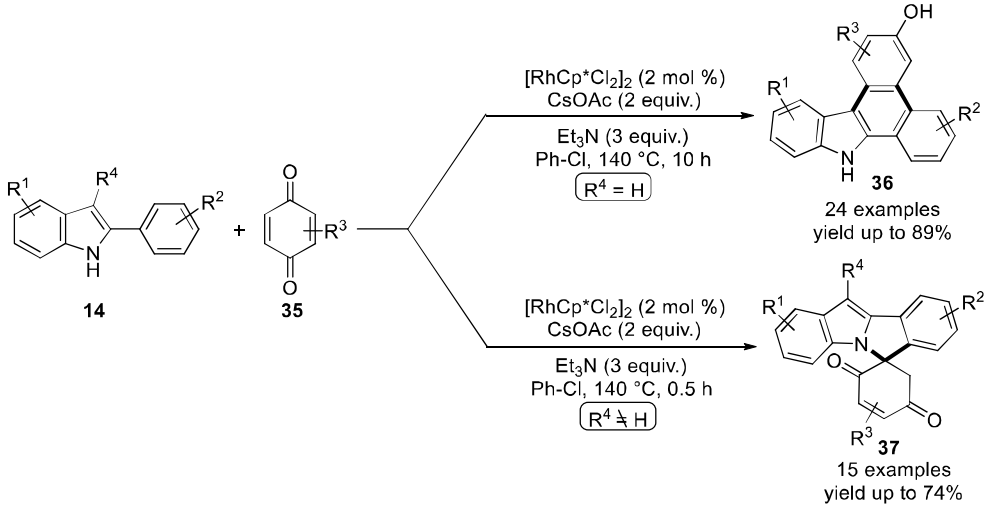

Scheme 3.3B.12 Rh(III)-catalyzed annulation and spiroannulation of 2-arylindoles with benzoquinone

In 2019, Szostak group reported the synthesis of indolo[1,2-*c*]quinazolines **(39)** by utilization of Rh(III)-catalyzed C–H amidation of 2-arylindoles **(14)** with dioxazolones **(38) (Scheme 3.3B.13)**.[59] The protocol involves C–H amidation and intramolecular N–H/N–C(O) cyclization in a mild and efficient manner, leading to the synthesis of indolo[1,2-*c*]quinazolines in good to excellent yields. The reaction showed broad substrate scope and high atom economy with removal of CO_2 and H_2O as byproducts. Intriguingly, the obtained cyclized products exhibit promising antitumor activity.

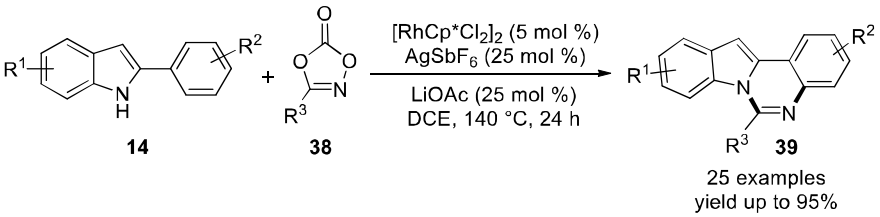

Scheme 3.3B.13 Rh(III)-catalyzed synthesis of indolo[1,2-*c*]quinazolines by coupling of 2-arylindoles with dioxazolones.

Cui *et al*. reported an efficient and novel strategy for the construction of furo[3,4-*c*]indolo[2,1-*a*]isoquinolines **(41)** *via* Rh(III)-catalyzed cascade C−H activation/annulation/lactonization of 2-arylindoles **(14)** with 4-hydroxy-2-alkynoates **(40)** **(Scheme 3.3B.14)**.[60] The promising advantages of the protocol are high efficiency and step economy, good functional group compatibility with excellent regioselectivity. The synthetic utility of the designed protocol was described that lactone converted into the thionolactone by using Lawesson reagent. The synthesized polycyclic furo[3,4-*c*]indolo[2,1-*a*]isoquinoline derivatives displayed fluorescent emission.

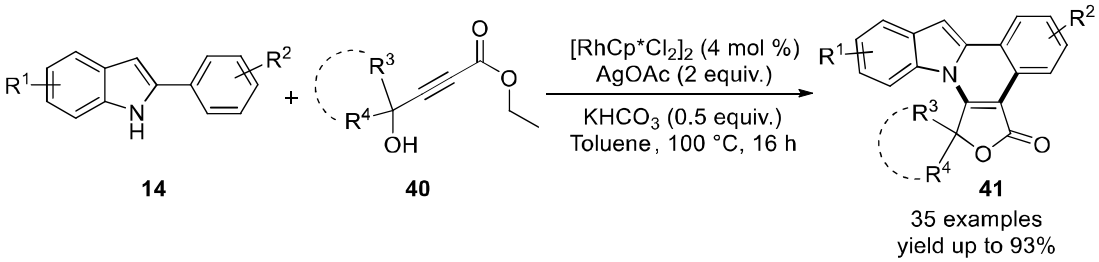

Scheme 3.3B.14 Rh(III)-catalyzed cascade reactions of 2-phenyl indoles with 4-hydroxy-2-alkynoates

As part of our interest in Rh(III)-catalyzed annulation reactions and the biological importance of 2-arylindoles **(14)** and maleimides **(2)**, we have developed a Rh(III)-catalyzed annulation and spirocyclization of 2-arylindoles with maleimides in the presence of for the formation of pyrrolo[3,4-*c*]carbazole-1,3(2*H*,8*H*)-dione **(42)** and spiro[isoindolo[2,1-*a*]indole-6,3'-pyrrolidine]-2',5'-dione **(46)** frameworks **(Scheme 3.3B.15)**. The method was also applied to 2-heteroarylindoles to prepare isogranulatimide alkaloid analogues.

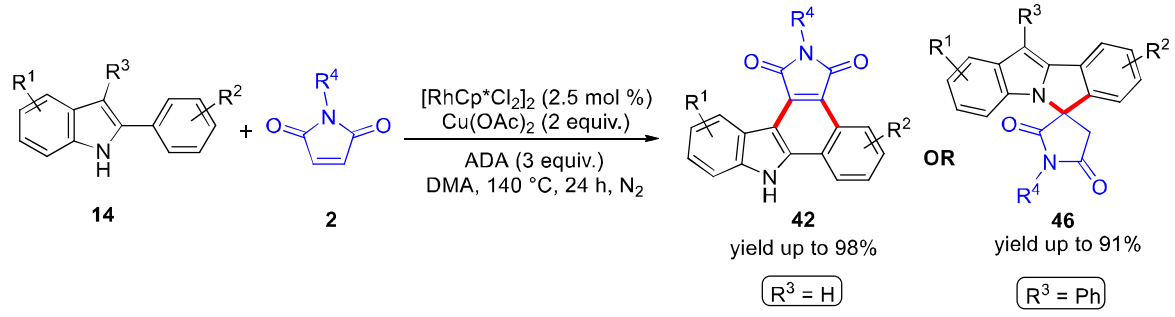

Scheme 3.3B.15 Rh(III)-catalyzed annulation and spirocyclization of 2-arylindoles with maleimides

3.3B.2 RESULTS AND DISCUSSION

Initial reaction of 2-phenylindole (**14a**) with *N*-methyl maleimide (**2a**) in the presence of $[RhCp^*Cl_2]_2$ (2.5 mol %) and $Cu(OAc)_2$ (2 equiv.) in DMF at 140 °C for 24 h gave annulated product, 2-methylbenzo[*a*]pyrrolo[3,4-*c*]carbazole-1,3-(2*H*,8*H*)-dione (**42aa**) in 15% yield (**Table 3.3B.2**, entry 1).[42] To improve the yield of **42aa**, various experiments were performed. Among different solvents such as DMSO, DMA, toluene, xylene, PhCl and DCE screened (**Table 3.3B.2**, entries 1-7), DMA was found to be the most suitable solvent for this reaction giving **42aa** in 38% yield. From screening of various oxidants (**Table 3.3B.2**, entries 8-10), $Cu(OAc)_2$ was found to be the most suitable oxidant. Other oxidants, AgOAc and Ag_2CO_3 led to lower yields of **42aa**, while IBD was ineffective. Metal catalysts such as $[Cp^*Co(CO)I_2]$, $[Ru(p\text{-cymene})Cl_2]_2$ and $Pd(OAc)_2$ were found less effective affording **42aa** in 25%, 10% and 21% yields, respectively (**Table 3.3B.2**, entries 11-13). Use of acidic additives such as PivOH, ADA and TsOH with $[RhCp^*Cl_2]_2$ and $Cu(OAc)_2$ in DMA improved yield of **42aa**, whereas basic additives such as CsOAc, NaOAc and Na_2CO_3 were ineffective (**Table 3.3B.2**, entries 14-19). Efforts in running the reaction at lower temperatures proved to be unfruitful, as **42aa** was obtained in 9% and 21% at 80 °C and 110 °C, respectively (**Table 3.3B.2**, entries 20-21). Reducing the loading of $[RhCp^*Cl_2]_2$ from 2.5 mol % to 1 mol % resulted decrease in the yield of **42aa** (**Table 3.3B.2**, entries 22-23). Interestingly, yield of **42aa** improved to 73% when combination of 3.0 equiv. of ADA was used as additive (**Table 3.3B.2**, entry 24). In addition, the desired product **42aa** was not obtained in the absence of $[RhCp^*Cl_2]_2$ (**Table 3.3B.2**, entry 25).

The structure of the **42aa** was fully elucidated by NMR and HRMS analysis. In ^1H NMR the C3 proton of the 2-phenylindole is totally disappeared and NH proton also shifted in deshielded region at δ 12.8 ppm. Moreover, the maleimides containing methyl protons appeared at δ 3.1 ppm. In ^{13}C NMR the two-carbonyl carbon of the maleimide observed at δ 169.6 ppm and δ 170.5 ppm as well as the methyl carbon at δ 24.0 ppm. The remaining protons and carbons of compound **42aa** were observed at their respective positions in ^1H and $^{13}C\{^1H\}$ NMR **(Figure 3.3B.2)**. In addition, peak at (*m/z*) 301.0981 in HRMS corresponding to $C_{19}H_{13}N_2O_2$ $[M + H]^+$ ion confirmed the structure of **42aa (Figure 3.3B.3)**.

Table 3.3B.1 Optimization of reaction conditions.[a]

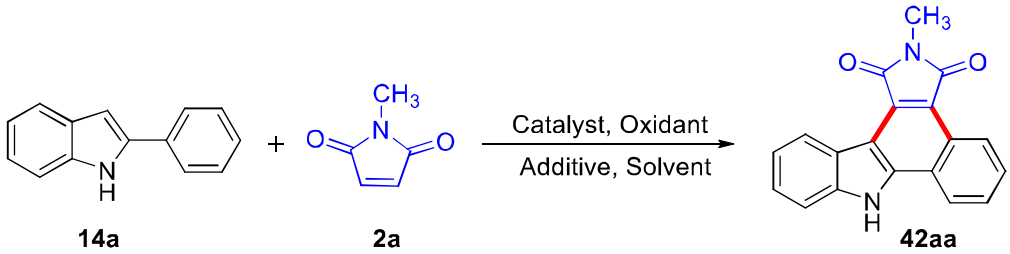

14a **2a** **42aa**

Entry	Catalyst	Oxidant	Additive	Solvent	Yield **42aa** (%)[b]
1	$[RhCp^*Cl_2]_2$	$Cu(OAc)_2$	-	DMF	15
2	$[RhCp^*Cl_2]_2$	$Cu(OAc)_2$	-	DMSO	20
3	$[RhCp^*Cl_2]_2$	$Cu(OAc)_2$	-	DMA	38
4	$[RhCp^*Cl_2]_2$	$Cu(OAc)_2$	-	Toluene	NR
6	$[RhCp^*Cl_2]_2$	$Cu(OAc)_2$	-	Xylene	NR
5	$[RhCp^*Cl_2]_2$	$Cu(OAc)_2$	-	PhCl	NR
7	$[RhCp^*Cl_2]_2$	$Cu(OAc)_2$	-	DCE	NR
8	$[RhCp^*Cl_2]_2$	AgOAc	-	DMA	15
9	$[RhCp^*Cl_2]_2$	Ag_2CO_3	-	DMA	24
10	$[RhCp^*Cl_2]_2$	IBD	-	DMA	NR
11	$[Cp^*Co(CO)I_2]$	$Cu(OAc)_2$	-	DMA	25
12	$[Ru(p\text{-cymene})Cl_2]_2$	$Cu(OAc)_2$	-	DMA	10
13	$Pd(OAc)_2$	$Cu(OAc)_2$	-	DMA	21
14	$[RhCp^*Cl_2]_2$	$Cu(OAc)_2$	PivOH	DMA	55
15	$[RhCp^*Cl_2]_2$	$Cu(OAc)_2$	ADA	DMA	59
16	$[RhCp^*Cl_2]_2$	$Cu(OAc)_2$	TsOH	DMA	45
17	$[RhCp^*Cl_2]_2$	$Cu(OAc)_2$	CsOAc	DMA	10
18	$[RhCp^*Cl_2]_2$	$Cu(OAc)_2$	NaOAc	DMA	15
19	$[RhCp^*Cl_2]_2$	$Cu(OAc)_2$	Na_2CO_3	DMA	NR
20	$[RhCp^*Cl_2]_2$	$Cu(OAc)_2$	ADA	DMA	9[c]
21	$[RhCp^*Cl_2]_2$	$Cu(OAc)_2$	ADA	DMA	21[d]
22	$[RhCp^*Cl_2]_2$	$Cu(OAc)_2$	ADA	DMA	52[e]
23	$[RhCp^*Cl_2]_2$	$Cu(OAc)_2$	ADA	DMA	53[f]
24	$[RhCp^*Cl_2]_2$	$Cu(OAc)_2$	ADA	DMA	73[f,g]
25	-	$Cu(OAc)_2$	ADA	DMA	NR

[a]Reaction conditions: **14a** (0.26 mmol), **2a** (0.52 mmol), catalyst (2.5 mol %), oxidant (2 equiv.), additive (3 equiv.), solvent (2 mL), 140 °C, N_2 atm., 24 h. [b]Isolated yields. [c]Reaction at 80 °C. [d]Reaction at 110 °C. [e]$[RhCp^*Cl_2]_2$ (1.0 mol %) was used. [f]$[RhCp^*Cl_2]_2$ (2.0 mol %) was used. [g]ADA (3.0 equiv.) was used. (ADA = 1-Adamantanecarboxylic acid)

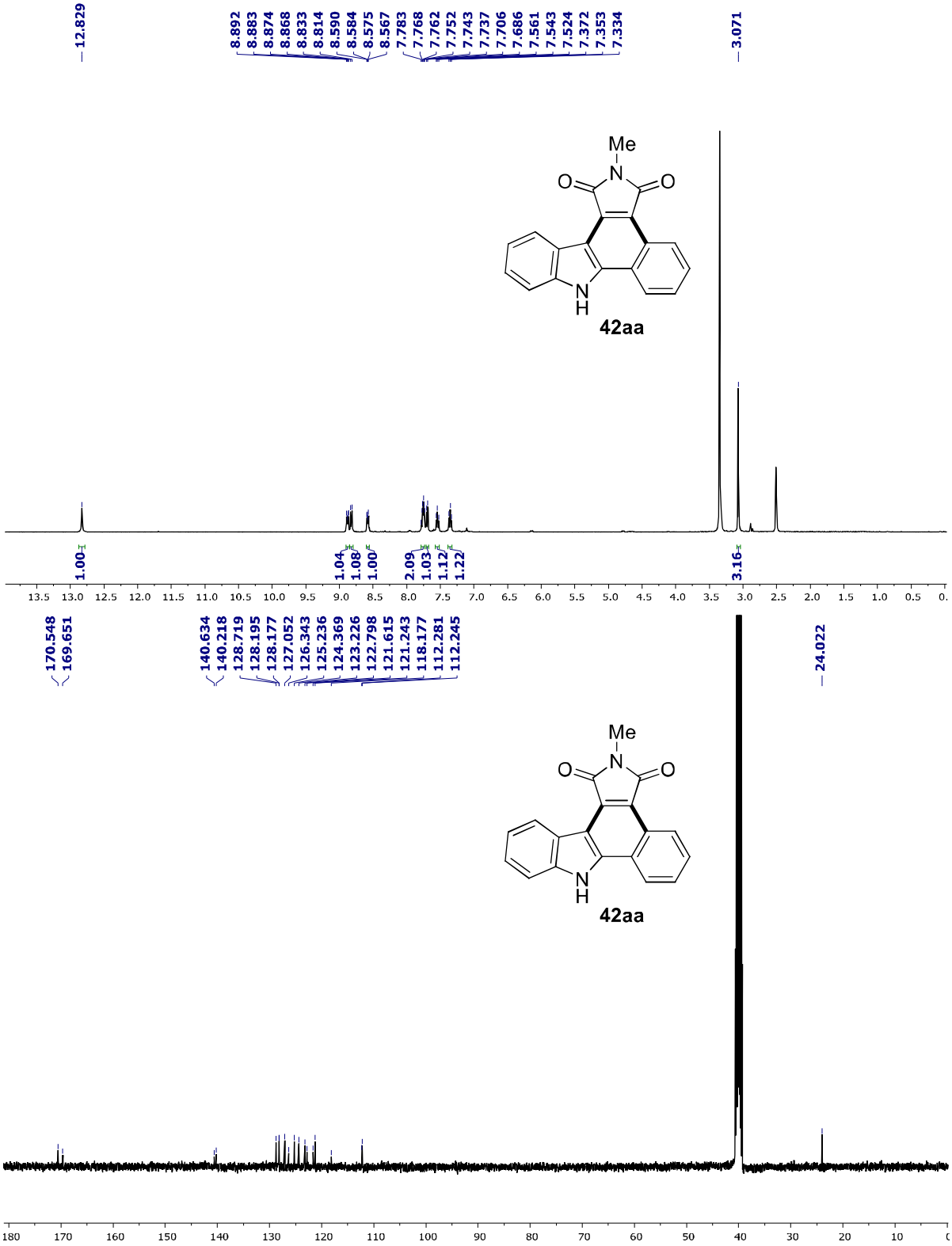

Figure 3.3B.2 ^{1}H and ^{13}C{^{1}H} NMR spectra of 2-methylbenzo[*a*]pyrrolo[3,4-*c*]carbazole-1,3(2*H*,8*H*)-dione (**42aa**) in DMSO-d_6

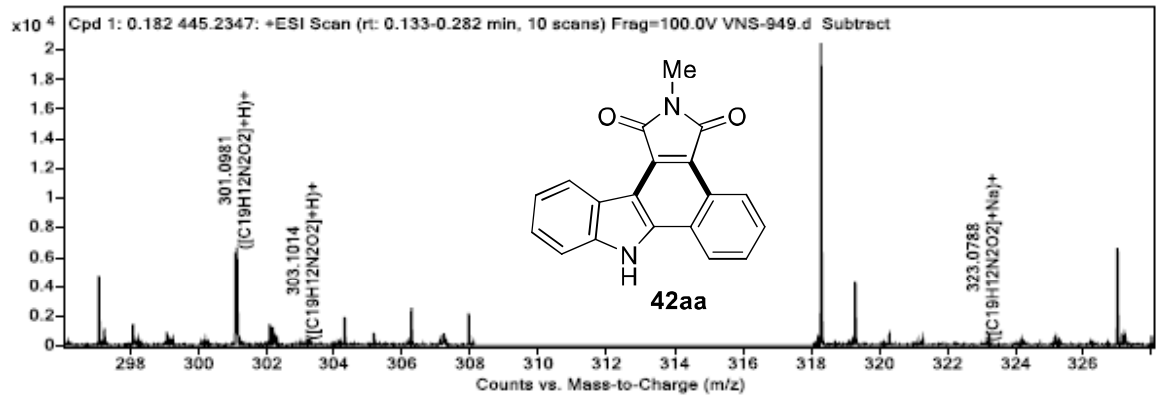

Figure 3.3B.3 HRMS spectrum of 2-methylbenzo[*a*]pyrrolo[3,4-*c*]carbazole-1,3(2*H*,8*H*)-dione (**42aa**)

With the optimized reaction conditions in hand, we examined the substrate scope for 2-arylindoles. As summarized in **Table 3.3B.2**, an array of 2-arylindoles with various functional groups such as Me, -CF_3, -F, -Br, -OMe, and -OH (**14a-m**) underwent successful annulation reaction with maleimide **2a** to afford desired products **42aa-42ma** in good to excellent yields (50-98%). It is worth mentioning that 2-arylindoles with electron withdrawing groups on C-2 aryl ring afforded higher yields of the annulated products (Compare **42ba** and **42fa** vs **42ca** and **42da**). 2-(2,4-Difluorophenyl)indole (**14j**) reacted with **2a** to afford corresponding annulated product **42ja** in almost quantitative yield (98%). Reaction of 2-arylindole with *meta*-substituents (**14h**) allowed C H activation to produce the products **42ha** with excellent regioselectivity in 97% yield. 2-(Naphthalen-1-yl)-1*H*-indole (**14l**) and 2-(thiophen-2-yl)-1*H*-indole (**14m**) also afforded desired products **42la** and **42ma** in 71% and 53% yields, respectively.

Next, we examined the substrate scope of maleimides under the optimal conditions. Maleimides with *N*-ethyl (**2b**), *N*-benzyl (**2c**), *N*-phenyl (**2d**), *N*-tolyl (**2e**), *N*-anisyl (**2f**), *N*-(4-bromobenzene) (**2g**), *N*-(4-nitrobenzene) (**2h**) and *N*-naphthyl (**2i**) groups underwent cyclization reaction with **1a** to afford the desired products **42ab**-**42ai** in moderate to good (43-75%) yields. Interestingly, maleimide with free NH (**2j**) also reacted with **14a** under these reaction conditions to afford corresponding product **42aj** in 61% yield. Structure of all the products was fully characterized by spectral analysis. Further, structure of **42ab** was unambiguously confirmed by single crystal X-ray analysis (CCDC No. 2024848).

The compound crystallized in Triclinic P-1 space group. One molecule along with one disordered solvent DMSO ($C_{20}H_{14}N_2O_2.C_2H_6SO$) appeared in the asymmetric unit. The fused polycyclic rings

of the molecule are closer to planar in nature. The N1—C8, N1—C1, N2—C17, N2—C18 and N2—C19 bond lengths are 1.3703(18), 1.3892(19), 1.3877(19), 1.4099(19) and 1.4619(18) Å respectively. The amide carbonyl bond lengths C17=O1 and C18=O2 are 1.2109(18) and 1.2070(19) Å respectively. The molecule is interacting with solvent DMSO through a hydrogen bonding N1—H----O=SMe_2 with a hydrogen bonding bond length of 2.056 Å between NH of indole as a donor with oxygen of DMSO as an acceptor.

Table 3.3B.2 Substrate scope for 2-arylindoles and maleimides.[a,b]

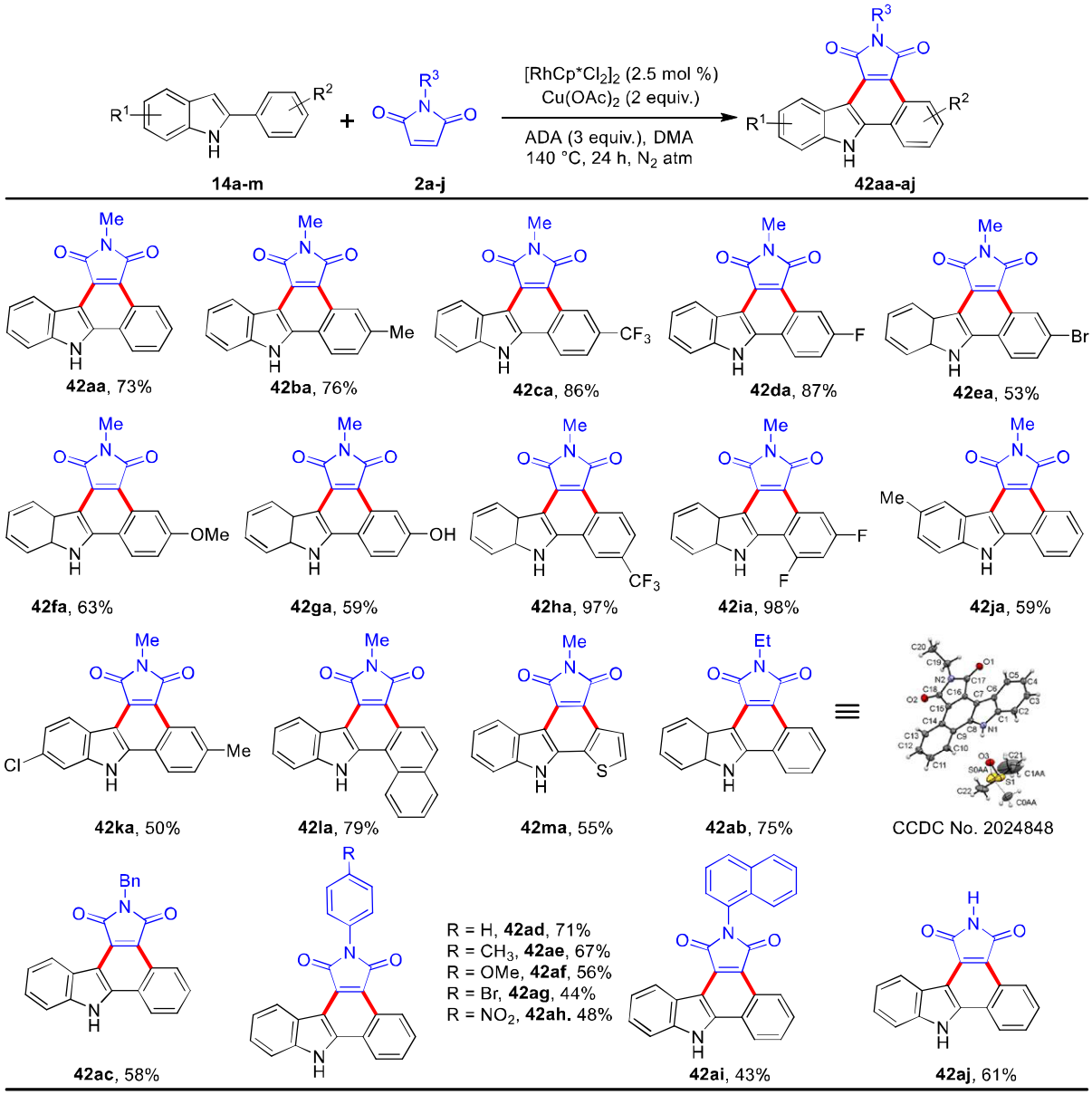

[a]Reaction conditions: **14** (0.26 mmol), **2** (0.52 mmol), $[RhCp^*Cl_2]_2$ (2.5 mol %), $Cu(OAc)_2$ (2 equiv.), ADA (3 equiv.), DMA (2 mL), 140 °C, N_2 atm., 24 h. [b]Isolated yields.

To further demonstrate synthetic utility of this method we performed gram-scale synthesis of **42aa** **(Scheme 3.3B.16)**. The reaction of **14a** (1 gm, 5.18 mmol) with **2a** (1.15 gm, 10.36 mmol) in presence of $[RhCp^*Cl_2]_2$ (80 mg, 0.13 mmol) performed in a standard condition to produced annulated product **42aa** in 72% yield. Thus, the annulation reaction proved scalable.

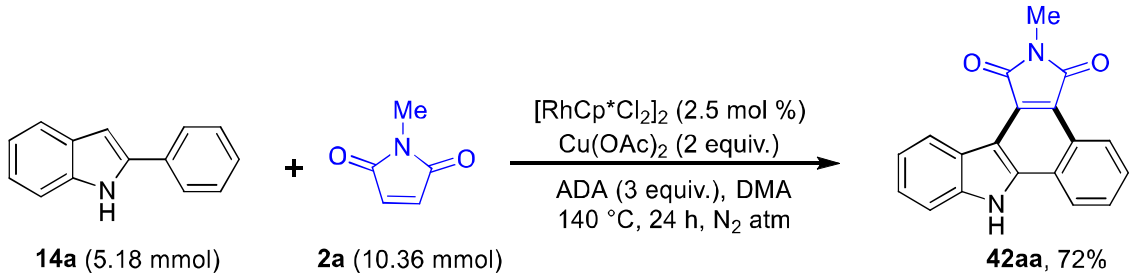

Scheme 3.3B.16 Gram-scale experiments.

After evaluating the substrate scope of this methodology, we explored the possibility of using 2-heteroarylindoles to access isogranulatimide alkaloid analogues. Granulatimides are natural alkaloids isolated from the Brazilian ascidian *Didemnum granulatum* that are found to exhibit Chk1 inhibition.[61-63] To our satisfaction reaction of 2-(1*H*-pyrazol-1-yl)-1*H*-indoles (**43a-d**) with **2a** under optimal reaction condition afforded corresponding annulated products **44aa**-**44da** in moderate to good (55-66%) yields **(Table 3.3B.3)**. The obtained annulated products were fully characterized by NMR and HRMS analysis. In the ^{1}H NMR of **44aa** two peaks of pyrazole protons appeared at δ 8.44 ppm and 7.09 ppm along with expected peaks for other protons **(Figure 3.3B.4)**. Likewise, maleimides carbonyl carbon peaks were observed at δ 168.7 ppm and 168.1 ppm in $^{13}C\{^1H\}$ NMR **(Figure 3.3B.5)**. Finally, presence of peak at *m/z* 291.0872 in HRMS corresponding to molecular formula $C_{16}H_{11}N_4O_2$ $[M + H]^+$ ion confirmed the structure of **44aa (Figure 3.3B.6)**. Likewise, the reaction of **43a** with other maleimides (**2b-d**) also afforded desired products **44ab-ad** in moderate to good (49-61%) yields. To our delight, reaction of maleimides **2j** with **43a** produced isogranulatimides analogues **44aj** in 47% yield. Further, the indolocarbazole-containing maleimide annulated bis-indole framework is found in natural products that possess a wide range of biological activities.[64-66] We performed the reaction of 2,3-bisindole **43d** with **2a** and **2j** under standard reaction conditions to obtain 7-methyl-5*H*-indolo[3,2-*a*]pyrrolo[3,4-*c*]carbazole-6,8(7*H*,13*H*)-dione **(44da)** and 5*H*-indolo[3,2-*a*]pyrrolo[3,4-*c*]carbazole-6,8-(7*H*,13*H*)-dione **(44dj)** in 68% and 56% yields, respectively **(Table 3.3B.3)**.

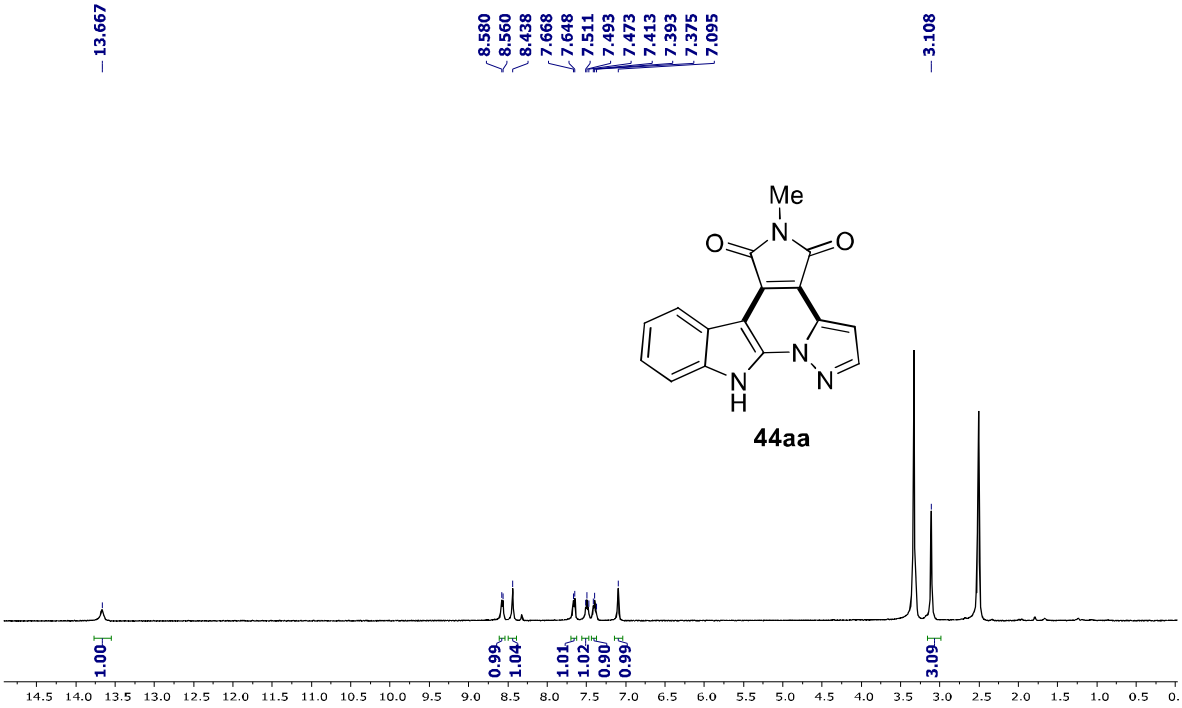

Figure 3.3B.4 ^{1}H NMR spectrum of 5-methylpyrazolo[1',5':1,6]pyrrolo[3',4':4,5]pyrido[2,3-*b*]indole-4,6(5*H*,11*H*)-dione **(44aa)** in DMSO-d_6

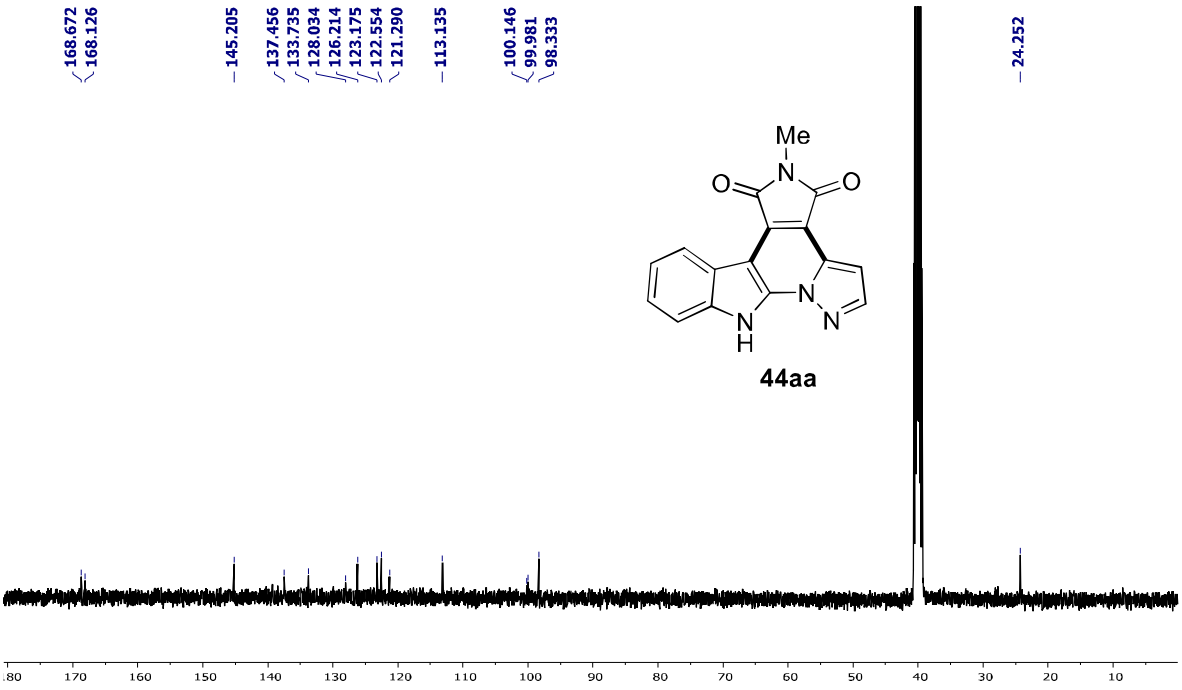

Figure 3.3B.5 ^{13}C NMR spectrum of 5-methylpyrazolo[1',5':1,6]pyrrolo[3',4':4,5]pyrido[2,3-*b*]indole-4,6(5*H*,11*H*)-dione **(44aa)** in DMSO-d_6

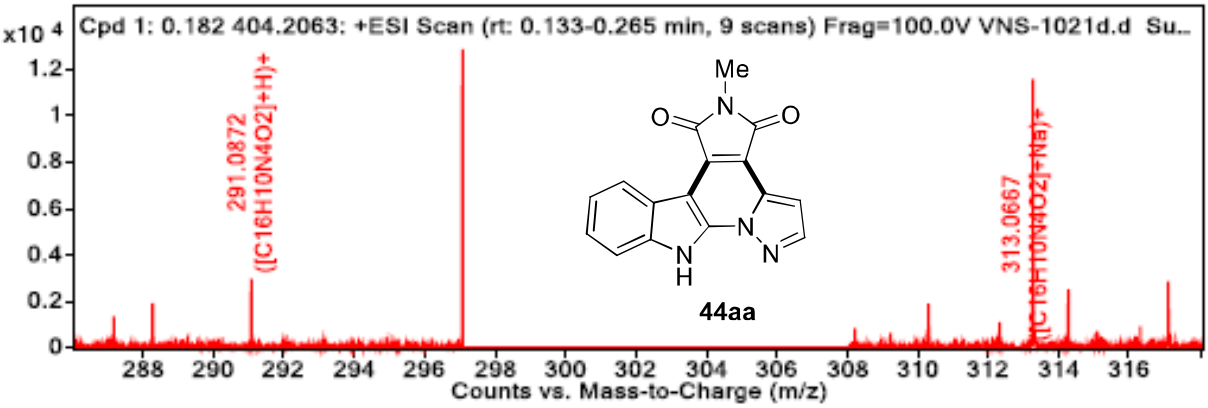

Figure 3.3B.6 HRMS spectrum of 5-methylpyrazolo[1',5':1,6]pyrrolo[3',4':4,5]pyrido[2,3-*b*]indole-4,6(5*H*,11*H*)-dione **(44aa)**

Table 3.3B.3 Substrate scope for 2-heteroarylindoles.[a,b]

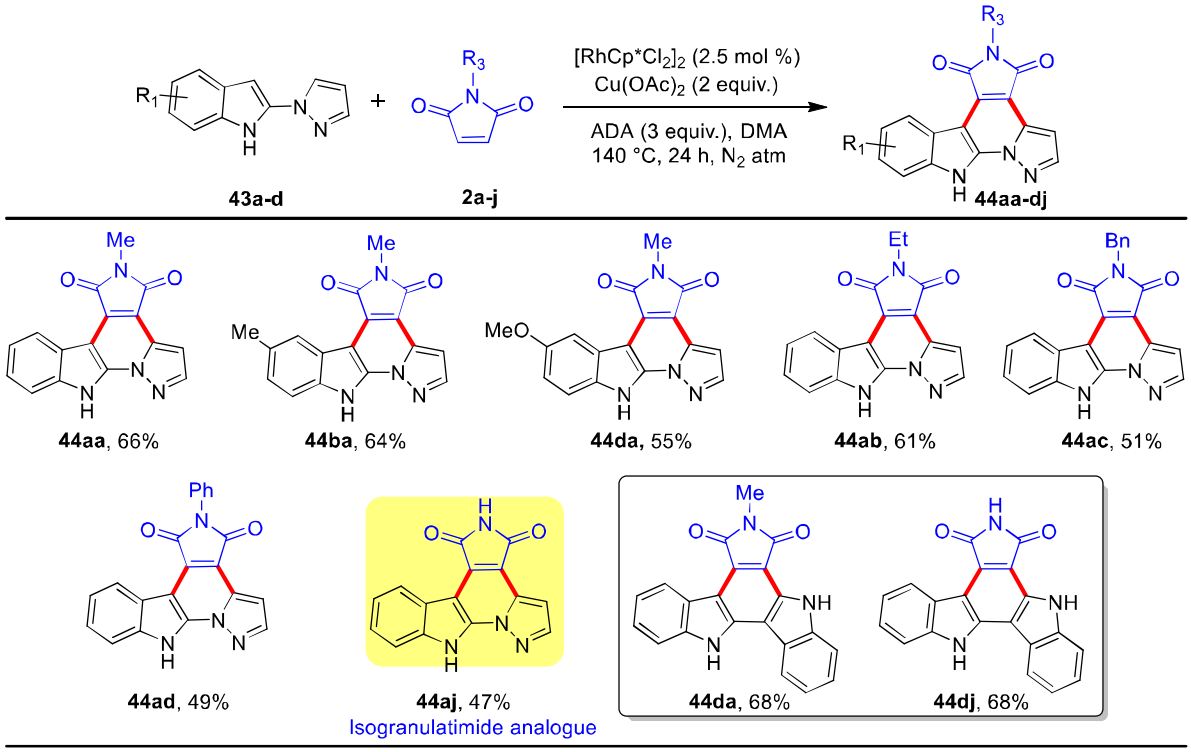

[a]Reaction conditions: **43** (0.26 mmol), **2** (0.52 mmol), $[RhCp^*Cl_2]_2$ (2.5 mol %), $Cu(OAc)_2$ (2 equiv.), ADA (3 equiv.), DMA (2 mL), 140 C, N_2 atm., 24 h. [b]Isolated yields.

To further extend the scope of this reaction, C-3 substituted indoles were reacted with maleimide under the optimal conditions (**Table 3.3B.4**). Interestingly, reaction of 2,3-diphenylindole (**45a**)

with **2a** in the presence of with $[RhCp^*Cl_2]_2$ and $Cu(OAc)_2$ in DMA afforded spiro product **46aa** in 91% yield.

The structure of obtained spiroannulated product **46aa** was ascertained by ^1H NMR, $^{13}C\{^1H\}$ NMR, and mass spectrometry analysis. In ^1H NMR of **46aa**, two-doublet were obtained at δ 3.70 ppm for -CH_2 group and a singlet at δ 3.51 ppm along with other aromatic protons. Further, appearance of two carbonyl carbon peaks were observed at 174.4 ppm and 173.9 ppm in the $^{13}C\{^1H\}$ NMR spectrum **(Figure 3.3B.7)** and a peak in the HRMS at *m/z* 423.1339 corresponding to molecular formula $C_{26}H_{19}N_2O_4$ $[M + HCOO]^-$ ion confirmed the structure of **46aa (Figure 3.3B.8)**.

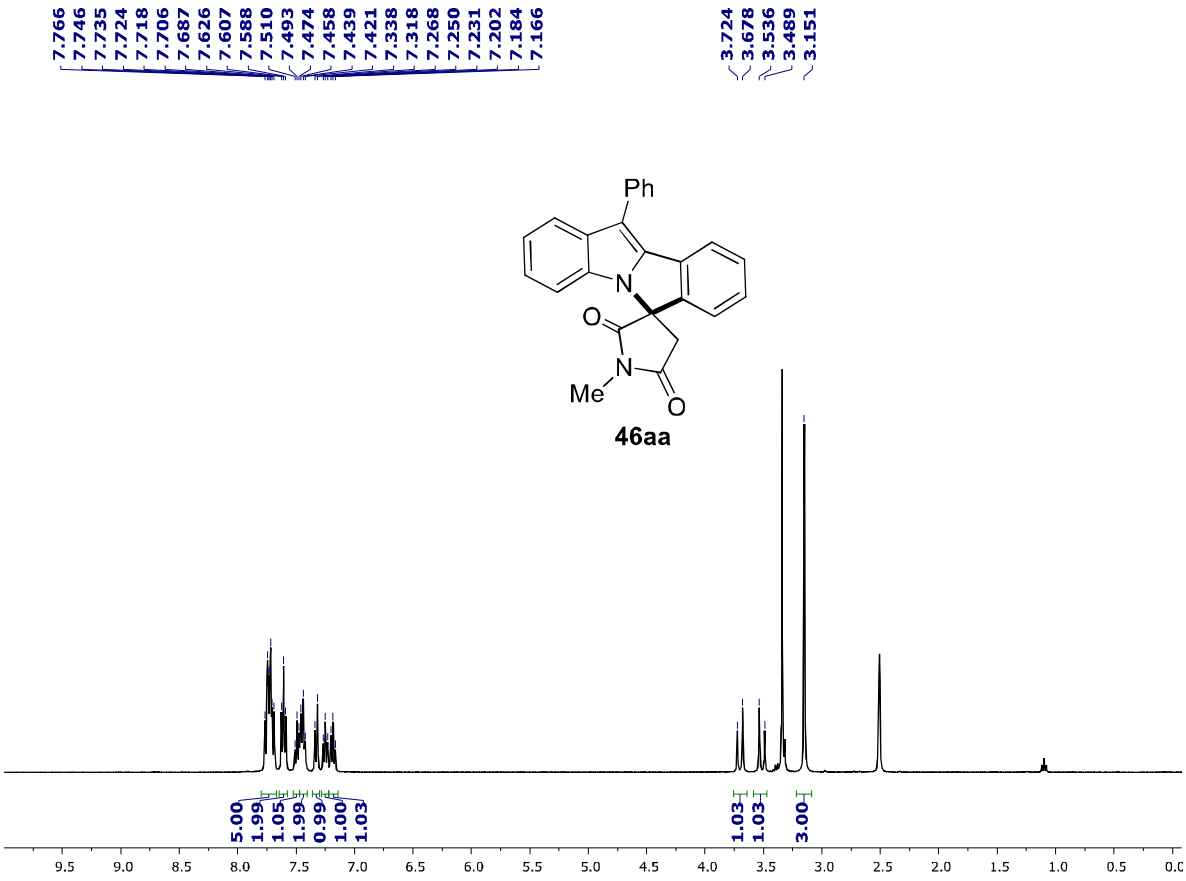

Figure 3.3B.7 ^1H NMR spectra of 1'-methyl-11-phenylspiro[isoindolo[2,1-*a*]indole-6,3'-pyrrolidine]-2',5'-dione **(46aa)** in DMSO-d_6

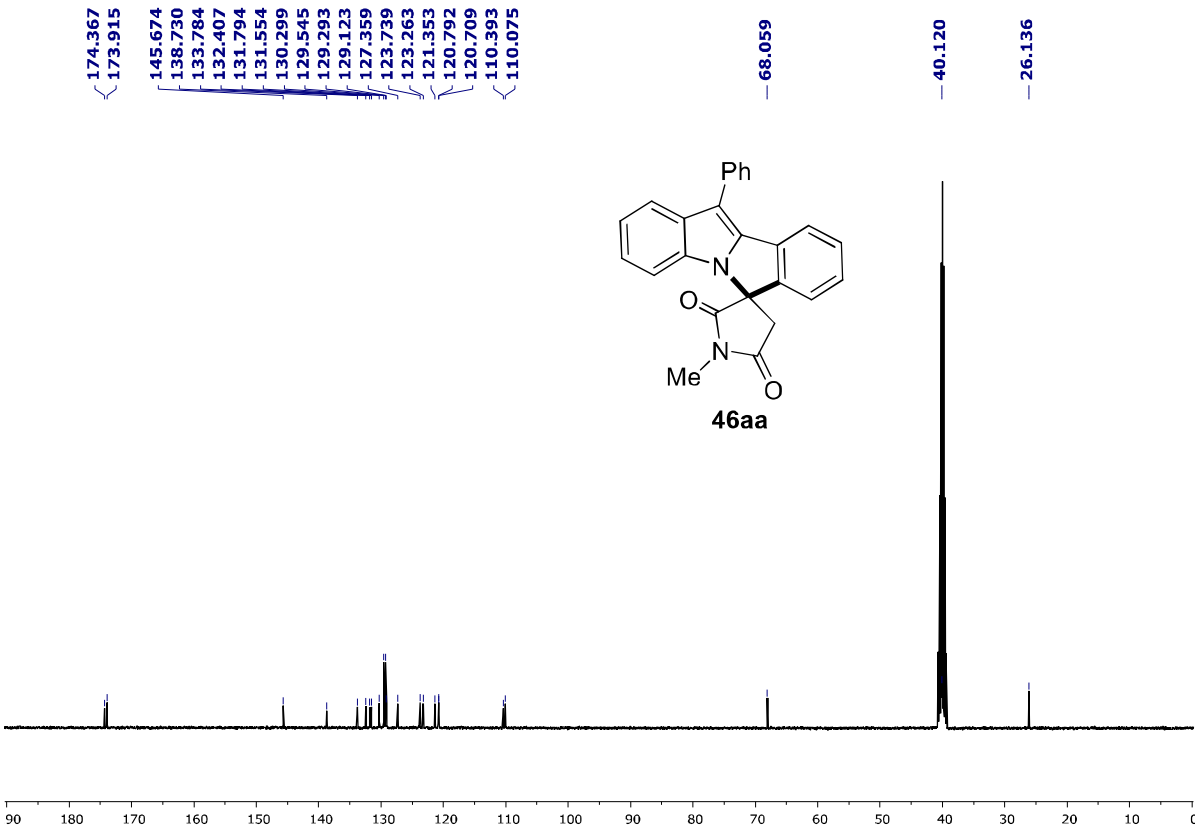

Figure 3.3B.8 $^{13}C\{^{1}H\}$ NMR spectra of 1'-methyl-11-phenylspiro[isoindolo[2,1-*a*]indole-6,3'-pyrrolidine]-2',5'-dione **(46aa)** in DMSO-d_6

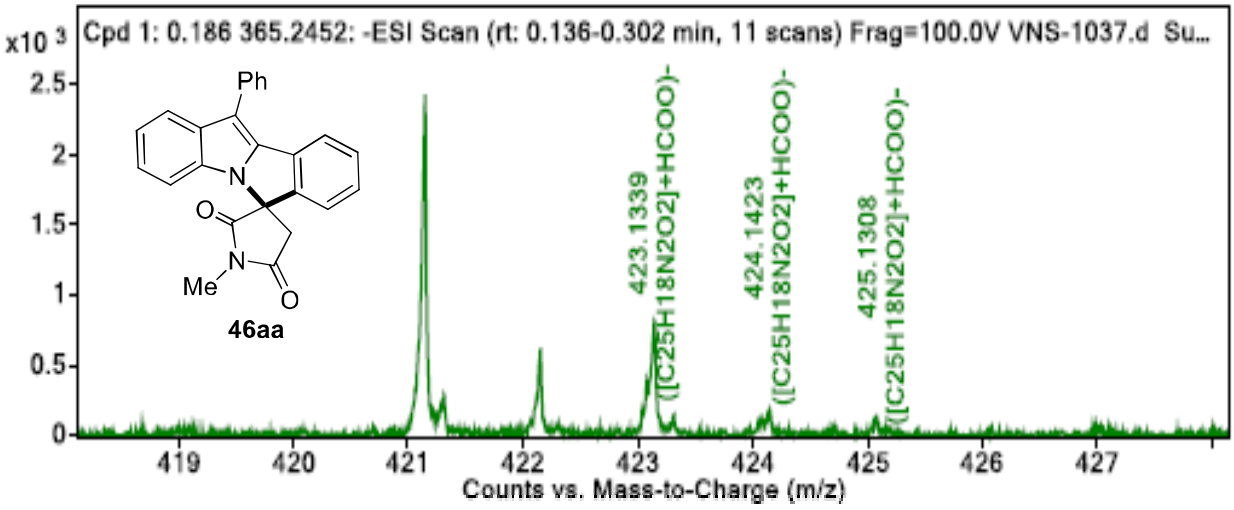

Figure 3.3B.9 HRMS spectrum of 1'-methyl-11-phenylspiro[isoindolo[2,1-*a*]indole-6,3'-pyrrolidine]-2',5'-dione **(46aa)**

Encouraged with this result, different 2,2-diphenylindoles (**45b-d**) were reacted with maleimides (**2a-d**) to afford corresponding spiro products **46ab-ad** in good to excellent (69-90%) yields.

Table 3.3B.4 Substrate scope for spirocylization of 2,3-diphenylindoles.[a,b]

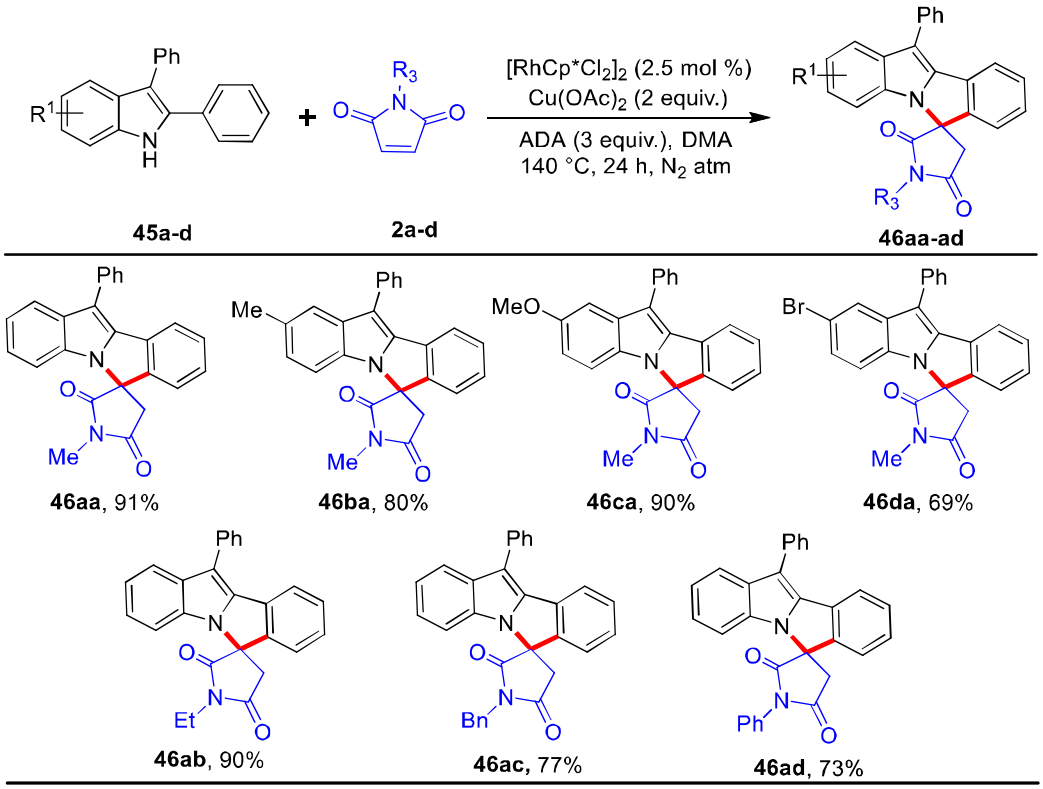

[a]Reaction conditions: **45** (0.26 mmol), **2** (0.52 mmol), $[RhCp^*Cl_2]_2$ (2.5 mol %), $Cu(OAc)_2$ (2 equiv.), ADA (3 equiv.), DMA (2 mL), 140 °C, N_2 atm., 24 h. [b]Isolated yields.

To gain better insight into the mechanism of the annulation reaction, a few control experiments were performed **(Scheme 3.3B.17)**. Firstly, effect of radical scavenger was studied by performing the reaction of **14a** with **2a** in presence of 2,2,6,6-tetramethylpiperidine-1-oxy (TEMPO) and butylated hydroxytoluene (BHT) **(Scheme 3.3B.17a)**. No significant reduction in the yield of **42aa** was observed, indicating that the reaction does not involve radical process. Reaction of *N*-methylindole (**47**) with **2a** failed to produce annulated product and **47** was recovered in 92% yield **(Scheme 3.3B.17b)**. This result demonstrated that free NH plays a significant role for the aryl C–H activation. Next competition experiment between differently substituted indoles (**14c** and **14f**) was carried out to delineate the action mode of the reaction **(Scheme 3.3B.17c)**. The result revealed that 2-arylindoles with electronically poor C-2 aryl ring (**14c**) was preferentially converted to

product (**42ca**/**42fa** = 3:1), suggesting C–H activation might occur *via* concerted metalation deprotonation (CMD) mechanism and not through Friedel-Crafts type electrophilic aromatic substitution mechanism. Further, the intermolecular kinetic isotopic effect (KIE) was defined on the basis of the competition reaction between **14a** and **14a-*d*$_5$** with **2a**, and KIE (P_H/P_D) value of ≃4.0 was observed. **(Scheme 3.3B.17d)**, pointing to a metalation/deprotonation reaction en route to the Rh(III) species.

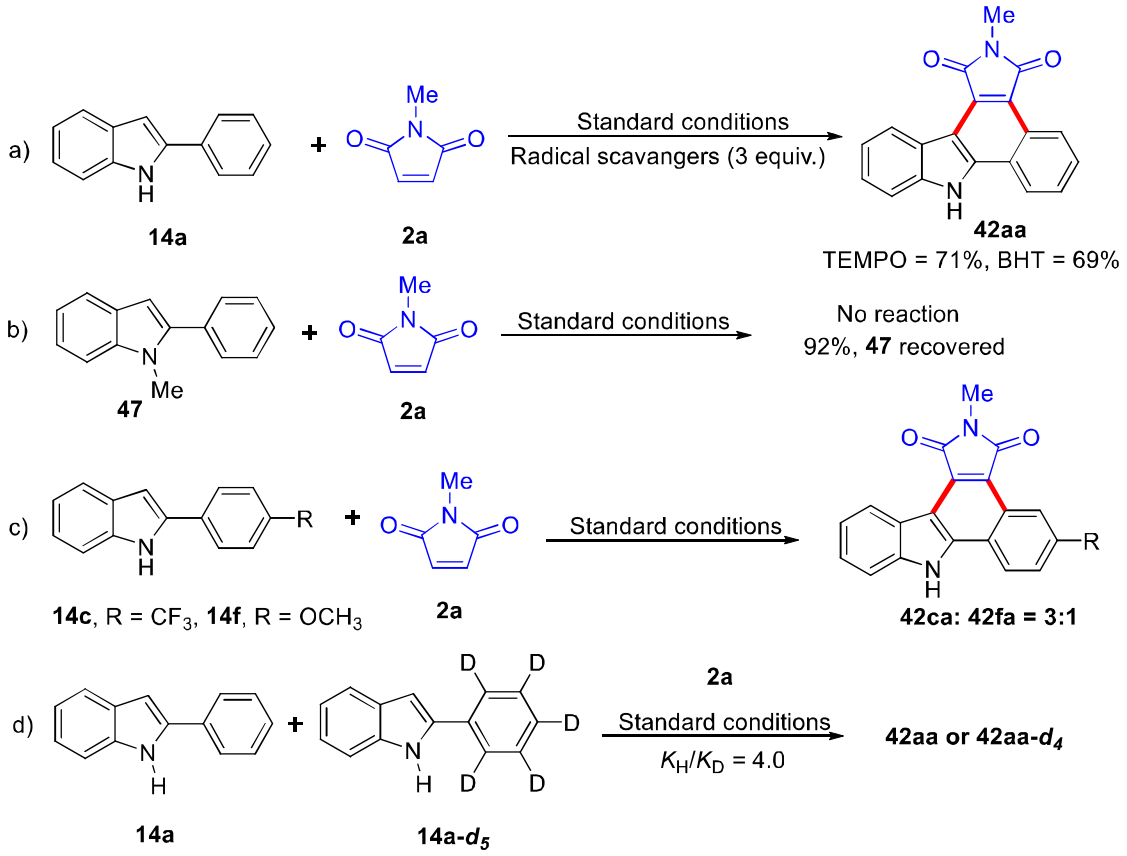

Scheme 3.3B.17 Control experiments.

Based on the experimental results and literature available,[67-70] a plausible mechanism of the reaction is proposed in **Scheme 3.3B.18**. Initially, Rh(III) coordinates with the nitrogen atom of indole (**14**/**45**) and then *ortho*-C–H bond cleavage of the aryl group *via* a concerted metalation–deprotonation (CMD) pathway gives rhodacycle **A** (detected in LC-HRMS 466.0856 $[M + H]^+$ from **14i**). Subsequently, co-ordination of maleimide (**2a**) with Rh(III) gives intermediate **B**, which undergoes migratory insertion to afford rhodacycle **C**. For indoles with unsubstituted C3-position (R^1 = H), rollover[71-73] of indole backbone and subsequent cyclometalative C–H

activation produces rhodacycle **D**. Reductive elimination produces intermediate **E** (detected in LC-HRMS 339.0905 $[M + H]^+$ from **14i**) and Rh(I) species. Oxidation of **E** produces annulated product **42aa**. For C3-substituted indoles (R1 = Ph), reductive elimination from rhodacycle **D** produces intermediate **F** (detected in LC-HRMS 379.1403 $[M + H]^+$ from **45a** and Rh(I) species. The nucleophilic addition takes place at C-3 position of maleimide moiety as it is more electrophilic than C-4 position. Thus, intermediate **F** instantaneously undergoes aza-Michael addition and forms spiro-product **46aa**. $Cu(OAc)_2$ oxidizes Rh(I) species to regenerate Rh(III) catalyst.

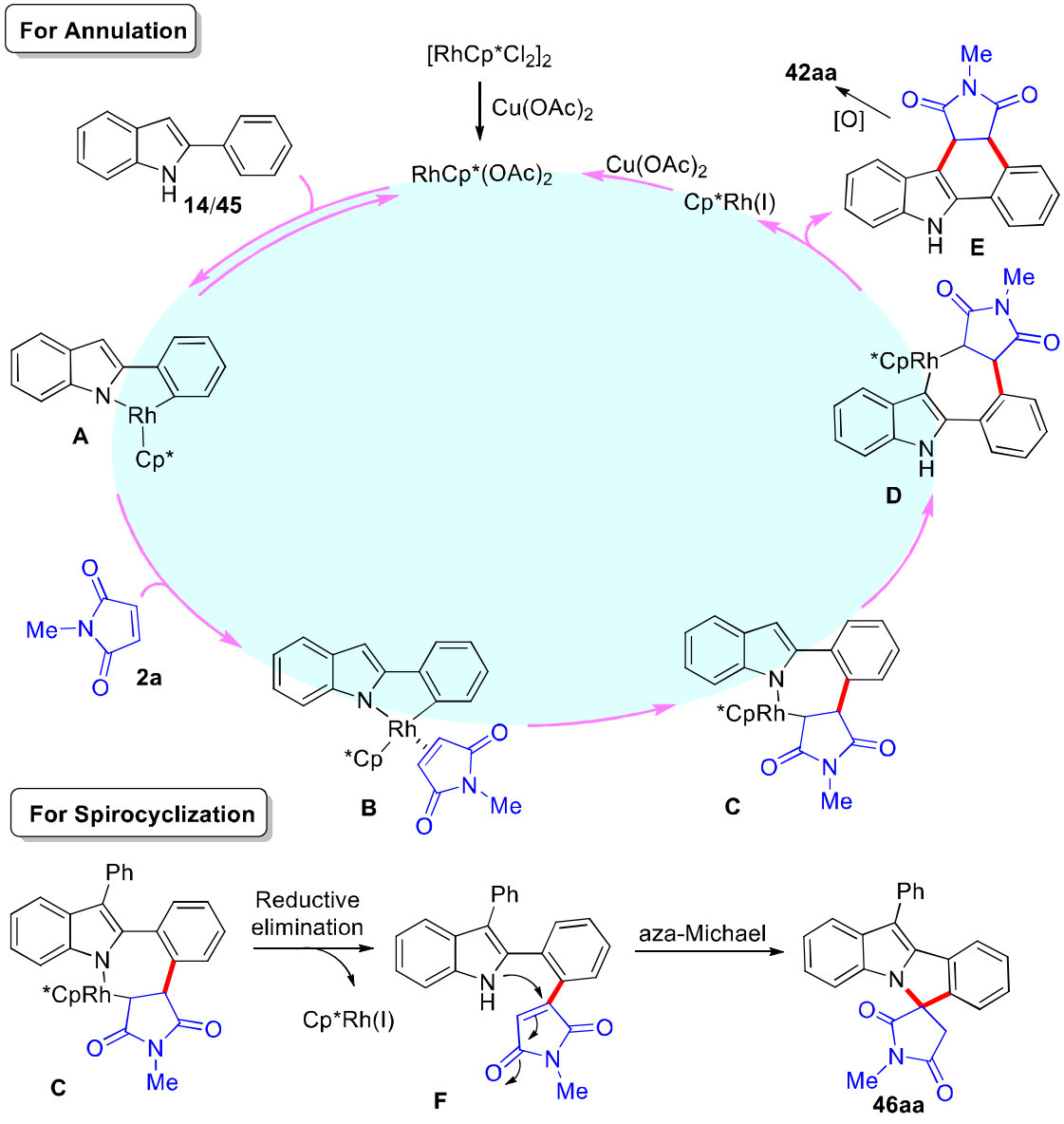

Scheme 3.3B.18 Proposed reaction mechanism.

The optical properties of **42** and **44** were also evaluated by recording absorption and emission spectra in DMSO (5×10^{-5} M) at room temperature (**Table 3.3B.5** and **Figure 3.3B.9**). The normalized absorption and emission spectra of **14a, 42aa** and **44aa** are shown in **Figure 3.3B.9**. The annulated compounds (**42** and **44**) exhibited absorption λ_{max} ($\pi^* \leftarrow \pi$) in the region 404 – 471 nm and emission 503 – 587 nm. A red shift in absorption and emission maxima was observed for annulated products. Interestingly, annulated product of 2-(1*H*-pyrazol-1-yl)-1*H*-indole (**43aa**) showed large red-shift as compare to that of 2-phenylindole **(14a)**.

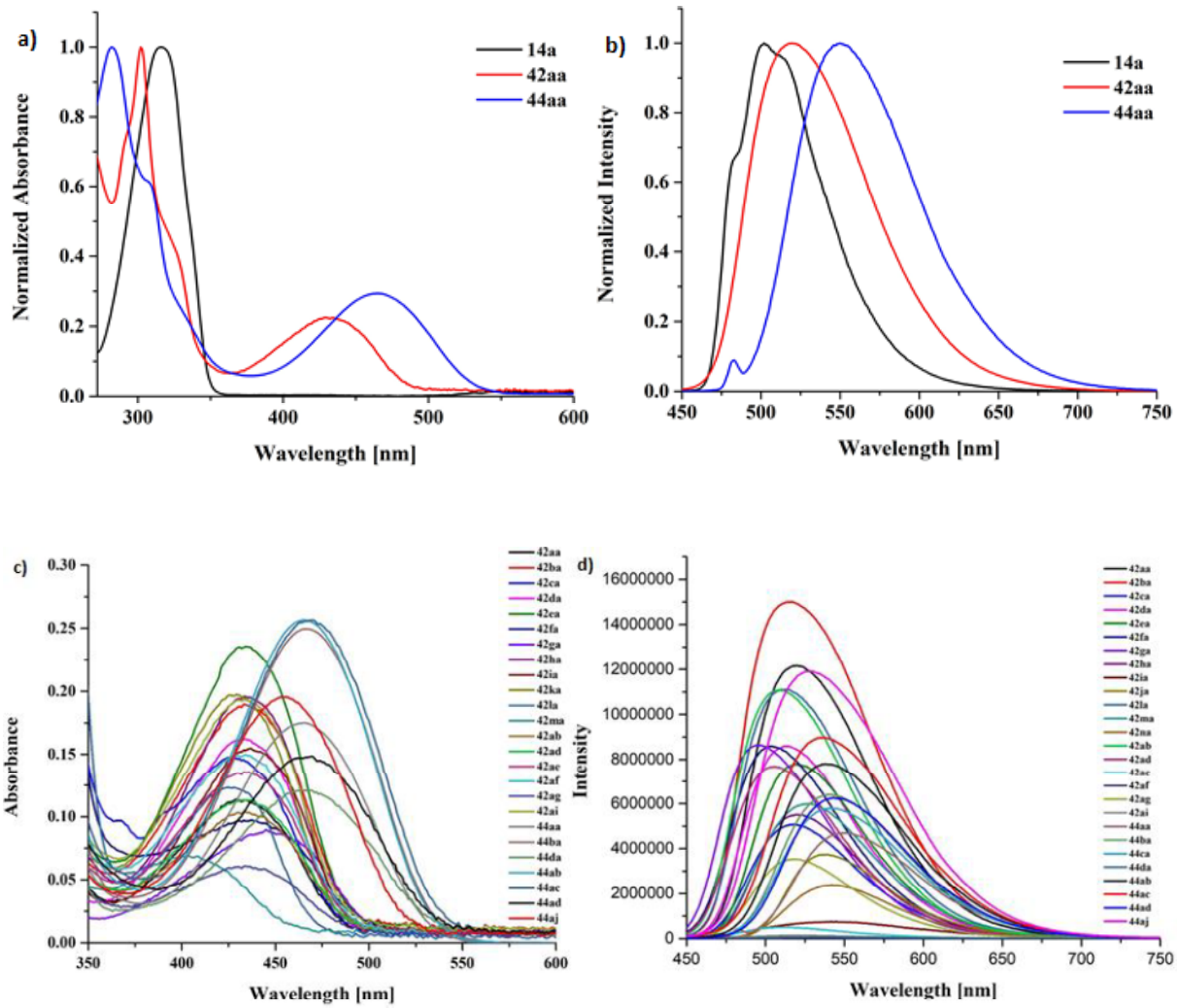

Figure 3.3B.10 Normalized a) UV-visible and b) emission spectra of **14a**, **42aa, 44aa** and representative c) UV-visible and d) emission spectra of **42** and **44** in DMSO.

Table 3.3B.5 Optical properties of 42 and 44:

Table 3.3B.5: UV-visible and fluorescence data for **42** and **44**

Compounds	$\lambda_{abs,\ max}$ (nm)	λ_{ex} (nm)	λ_{em} (nm)	Stokes shift cm^{-1} (nm)	ε^a ($M^{-1}cm^{-1}$)
14a	315	305	375	5079 (60)	18206
42aa	432	420	514	3693 (82)	3791
42ba	434	425	518	3736 (84)	6039
42ca	429	425	517	3968 (88)	4031
42da	433	425	513	3602 (80)	5115
42ea	434	420	514	3586 (80)	6175
42fa	442	430	520	3394 (78)	3001
42ga	448	440	521	3128 (73)	2822
42ha	435	420	517	3646 (82)	5372
42ia	438	390	511	3262 (73)	4612
42ka	429	425	513	3817 (84)	5730
42la	426	410	512	3943 (86)	3552
42ma	404	385	503	4872 (99)	3465
42ab	434	430	514	3586 (80)	3276
42ad	433	425	513	3602 (80)	3142
42ae	433	420	522	3938 (89)	3692
42af	432	425	517	3806 (85)	3861
42ag	436	430	524	3852 (88)	1376
42ai	432	420	516	3768 (84)	4703
44aa	466	460	569	3885 (103)	6160
44ba	466	455	571	3946 (105)	8210
44da	465	455	570	3962 (105)	3811
44ab	464	455	571	4039 (107)	8521
44ac	469	460	571	3809 (102)	7058
44ad	467	455	576	4052 (109)	4256
44aj	455	450	554	3927 (99)	7167

[a]All spectra measured in DMSO solution (1.0×10^{-5} M) at 25 °C.

3.3B.3 CONCLUSIONS

In summary, a Rh(III)-catalyzed dehydrogenative annulation and spirocyclization of 2-arylindoles with maleimides has been developed. An array of annulated and spirocycle indole derivatives were prepared in good to excellent yields. The protocol displays a broad scope with respect to both the indoles and maleimides, has high functional group tolerance, and is scalable. Additionally, annulation of 2-heteroarylindoles with maleimides under the optimized reaction conditions afforded isogranulatimide alkaloid analogues in moderate yields. The synthesized products were further explored for photophysical studies. The annulated products of series **44** showed high absorption and emission values as well as Stokes shifts value compare to the annulated products **42**.

3.3B.4 EXPERIMENTAL SECTION

3.3B.4.1 General Materials and Methods

Unless otherwise mentioned, all chemicals and solvents were commercially available and were used without further purification. 2-Arylindoles[74-75] and 2-(1*H*-pyrazol-1-yl)-1*H*-indole[76] derivatives are known compounds and synthesized by using reported methods. The ^{1}H NMR and ^{13}C NMR spectra were recorded on 400 MHz spectrometer. The coupling constant (J) values are given in Hz and δ values in ppm. The chemical multiplicities abbreviated as: singlet (s), doublet (d), triplet (t), quartet (q), quintet (quint), sextet (sext), septet (sept) and multiplet (m) and their combinations of them as well. For column chromatography silica gel (100-200 mesh size) was used. Thin-layer chromatography (TLC) were performed on commercially available 0.25 mm silica gel 60-F254 plate. Melting point were measured on an automated apparatus and are uncorrected. HRMS were reported using electrospray ionization (ESI) method on a TOF LC-MS spectrometer. The photophysical (absorption and fluorescence) studies were carried out using spectrophotometric grade DMSO and deionized water.

3.3B.4.2 General procedure for synthesis of 42, 44 and 46. A 10 mL pressure tube equipped with magnetic stir bar was charged with 2-(hetero)arylindoles (0.26 mmol) and *N*-substituted maleimides (0.52 mmol), $[Cp^*RhCl_2]_2$ (4 mg, 2.5 mol %), $Cu(OAc)_2$ (94 mg, 0.52 mmol), ADA (180 mg, 0.78 mmol) and DMA (2 mL). The reaction mixture was purged with nitrogen for 15 min, then reaction vial was caped and stirred at 140 ℃ in an oil bath for 24 h. After complete

consumption of starting materials on TLC, reaction mixture was cooled to room temperature, diluted by EtOAc (10 mL) and washed with chilled water (2 x 5 mL). The combined organic layer was dried over anhydrous Na_2SO_4, and concentrated under reduced pressure. The resulting residue was purified by column chromatography on size silica gel with EtOAc/hexane eluent to afford the desired products **42**, **44,** and **46**.

2-Methylbenzo[*a*]pyrrolo[3,4-*c*]carbazole-1,3(2*H*,8*H*)-dione (42aa): Orange solid (56 mg, 73%); R_f = 0.4 (EtOAc/Hexane = 1: 3, *v/v*); mp = 356-358 °C; ^{1}H NMR (400 MHz, DMSO-d_6) δ 12.83 (s, 1H), 8.89 – 8.87 (m, 1H), 8.82 (d, *J* = 7.6 Hz, 1H), 8.59 – 8.57 (m, 1H), 7.78 – 7.74 (m, 2H), 7.70 (d, *J* = 8.0 Hz, 1H), 7.54 (t, *J* = 7.0 Hz, 1H), 7.35 (t, *J* = 7.6 Hz, 1H), 3.07 (s, 3H); ^{13}C{^{1}H} NMR (100 MHz, DMSO-d_6) δ 170.6, 169.7, 140.6, 140.2, 128.7, 128.2, 128.2, 127.1, 126.3, 125.2, 124.4, 123.2, 122.8, 121.6, 121.2, 118.2, 112.3, 112.2, 24.0; HRMS (ESI) *m/z*: $[M + H]^+$ calculated for $C_{19}H_{13}N_2O_2^+$, 301.0972; found, 301.0981.

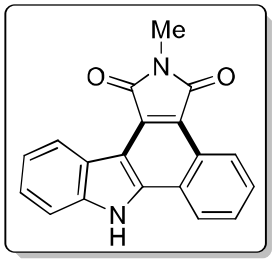

2,5-Dimethylbenzo[*a*]pyrrolo[3,4-*c*]carbazole-1,3(2*H*,8*H*)-dione (42ba): Yellow solid (57 mg, 76%); R_f = 0.4 (EtOAc/Hexane = 1: 4, *v/v*); mp 315-317 °C; ^{1}H NMR (400 MHz, DMSO-d_6) δ 12.76 (s, 1H), 8.83 (d, *J* = 8.0 Hz, 1H), 8.64 (s, 1H), 8.47 (d, *J* = 8.8 Hz, 1H), 7.68 (d, *J* = 8.0 Hz, 1H), 7.59 (d, *J* = 8.4, 1H), 7.53 (t, *J* = 7.6 Hz, 1H), 7.35 (t, *J* = 7.4 Hz, 1H), 3.07 (s, 3H), 2.55 (s, 3H); ^{13}C{^{1}H} NMR (100 MHz, DMSO-d_6) δ 170.5, 169.6, 140.9, 140.3, 138.4, 130.0, 128.1, 126.8, 126.6, 124.3, 124.1, 123.0, 121.7, 121.1, 120.9, 117.4, 112.2, 111.9, 23.9, 22.2; HRMS (ESI) *m/z*: $[M + H]^+$ calculated for $C_{20}H_{15}N_2O_2^+$, 315.1128; found, 315.1110.

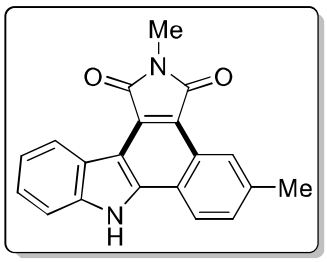

2-Methyl-5-(trifluoromethyl)benzo[*a*]pyrrolo[3,4-*c*]carbazole-1,3(2*H*,8*H*)-dione (42ca): Red solid (60 mg, 86%); R_f = 0.2 (EtOAc/Hexane = 1: 3, *v/v*); mp = 299-301 °C; ^{1}H NMR (400 MHz, DMSO-d_6) δ 13.05 (s, 1H), 9.14 (s, 1H), 8.79 – 8.73 (m, 2H), 8.01 (d, *J* = 8.8 Hz, 1H), 7.71 (d, *J* = 8.0 Hz, 1H), 7.59 (t, *J* = 7.6 Hz, 1H), 7.38 (t, *J* = 7.6 Hz, 1H), 3.05 (s, 3H); ^{13}C{^{1}H} NMR (100 MHz, DMSO-d_6) δ 169.9, 168.8, 140.5, 139.8, 129.0, 128.3, 128.0, 127.6, 124.7 (d, *J* = 1.7 Hz), 124.5, 123.8, 123.1, 123.1, 122.4, 121.5,

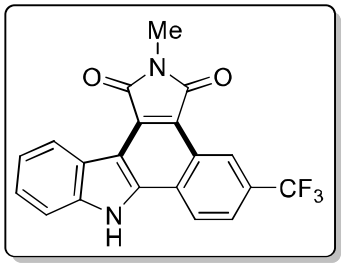

121.2, 118.2, 113.6, 112.4, 23.9; HRMS (ESI) *m/z*: $[M + H]^+$ calculated for $C_{20}H_{12}F_3N_2O_2^+$, 369.0845; found, 369.0836.

5-Fluoro-2-methylbenzo[*a*]pyrrolo[3,4-*c*]carbazole-1,3(2*H*,8*H*)-dione (42da): Green solid (65 mg, 87%); R_f = 0.3 (EtOAc/Hexane = 1: 4, *v/v*); mp = 321-323 °C; ^{1}H NMR (400 MHz, DMSO-d_6) δ 12.71 (s, 1H), 8.67 (d, *J* = 7.6 Hz, 1H), 8.49 – 8.46 (m, 1H), 8.26 (d, *J* = 10.8 Hz, 1H), 7.60 (d, *J* = 8.0 Hz, 1H), 7.58 – 7.50 (m, 2H), 7.31 (t, *J* = 7.4 Hz, 1H), 2.93 (s, 3H); ^{13}C{^{1}H} NMR (100 MHz, DMSO-d_6) δ 170.1, 169.2, 160.6, 140.9, 140.3, 129.0, 127.1, 126.3, 124.3, 121.4 (d, *J* = 9.1 Hz), 119.7, 117.9, 117.6, 117.2 (d, *J* = 5.0 Hz), 112.2, 112.1, 108.9, 108.6, 23.9; HRMS (ESI) *m/z*: $[M + H]^+$ calculated for $C_{19}H_{12}FN_2O_2^+$, 319.0877; found, 319.0874.

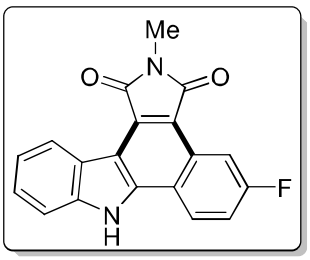

5-Bromo-2-methyl-8*a*,12*a*-dihydrobenzo[*a*]pyrrolo[3,4-*c*]carbazole-1,3(2*H*,8*H*)-dione (42ea): Yellow solid (35 mg, 53%); R_f = 0.41 (EtOAc/Hexane = 1: 6, *v/v*); mp = 290-292 °C; ^{1}H NMR (400 MHz, DMSO-d_6) δ 12.81 (s, 1H), 8.88 – 8.80 (m, 1H), 8.72 – 8.65 (m, 1H), 8.38 (d, *J* = 9.0 Hz, 1H), 7.81 – 7.75 (m, 1H), 7.70 – 7.63 (m, 1H), 7.54 (t, *J* = 7.6 Hz, 1H), 7.35 – 7.32 (m, 1H), 2.96 (s, 3H); ^{13}C{^{1}H} NMR (100 MHz, DMSO-d_6) δ 169.9, 168.9, 140.1, 133.5, 130.6, 128.6, 128.1, 127.2, 127.0, 126.8, 126.5, 125.2, 124.3, 123.6, 123.2, 121.4, 116.7, 112.2, 23.9; HRMS (ESI) *m/z*: $[M + H]^+$ calculated for $C_{19}H_{12}BrN_2O_2^+$, 379.0077; found, 379.0146.

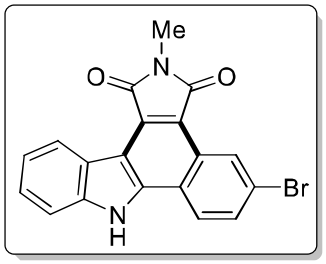

5-Methoxy-2-methylbenzo[*a*]pyrrolo[3,4-*c*]carbazole-1,3(2*H*,8*H*)-dione (42fa): Yellow solid (47 mg, 63%); R_f = 0.5 (EtOAc/Hexane = 1: 6, *v/v*); mp = 311-313 °C; ^{1}H NMR (400 MHz, DMSO-d_6) δ 12.57 (s, 1H), 8.73 (d, *J* = 7.6 Hz, 1H), 8.38 (d, *J* = 9.2 Hz, 1H), 8.08 (d, *J* = 2.8 Hz, 1H), 7.62 (d, *J* = 8.4 Hz, 1H), 7.49 (t, *J* = 7.4 Hz, 1H), 7.33 – 7.29 (m, 2H), 3.88 (s, 3H), 2.97 (s, 3H); ^{13}C{^{1}H} NMR (100 MHz, DMSO-d_6) δ 170.3, 169.3, 159.4, 141.2, 140.3, 128.0, 128.0, 126.6, 124.7, 124.2, 121.7, 120.9, 119.6, 117.5, 116.4, 111.9, 111.3, 103.8, 55.6, 23.7; HRMS (ESI) *m/z*: $[M + H]^+$ calculated for $C_{20}H_{15}N_2O_3^+$, 331.1077; found, 331.1037.

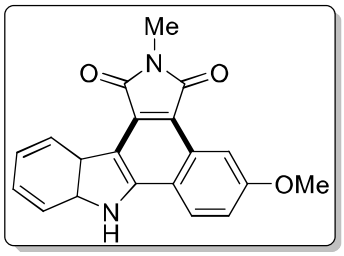

5-Hydroxy-2-methylbenzo[*a*]pyrrolo[3,4-*c*]carbazole-1,3(2*H*,8*H*)-dione (42ga): Red solid (45

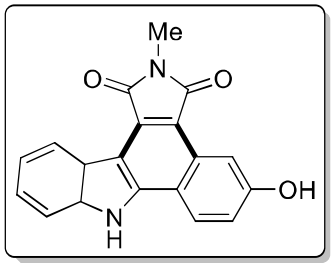

mg, 59%); R_f = 0.4 (EtOAc/Hexane = 1: 3, *v/v*); mp = 341-343 °C); ^{1}H NMR (400 MHz, DMSO-d_6) δ 12.69 (s, 1H), 10.37 (s, 1H), 8.84 (d, *J* = 9.2 Hz, 1H), 8.51 (d, *J* = 9.2 Hz, 1H), 8.31 (d, *J* = 2.4 Hz, 1H), 7.67 (d, *J* = 8.4 Hz, 1H), 7.51 (t, *J* = 7.6 Hz, 1H), 7.36 – 7.32 (m, 2H), 3.12 (s, 3H); ^{13}C{^{1}H} NMR (100 MHz, DMSO-d_6) δ 170.7, 169.8, 158.2, 141.7, 140.3, 128.6, 128.5, 126.5, 125.1, 124.1, 121.9, 121.0, 120.2, 117.0, 116.5, 112.0, 110.9, 107.2, 24.0; HRMS (ESI) *m/z*: $[M + H]^+$ calculated for $C_{19}H_{13}N_2O_3^+$, 317.0921; found, 317.0897.

2-Methyl-6-(trifluoromethyl)-8*a*,12*a*-dihydrobenzo[*a*]pyrrolo[3,4-*c*]carbazole-1,3(2*H*,8*H*)-

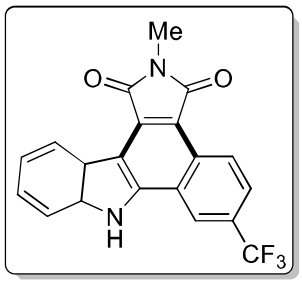

dione (42ha): Yellow solid (68 mg, 97%); R_f = 0.3 (EtOAc/Hexane = 1: 4, *v/v*); mp = 321-323 °C; ^{1}H NMR (400 MHz, DMSO-d_6) δ 12.84 (s, 1H), 8.83 (s, 1H), 8.79 (d, *J* = 8.8 Hz, 1H), 8.59 (d, *J* = 8.0 Hz, 1H), 7.83 (d, *J* = 8.8 Hz, 1H), 7.58 (d, *J* = 8.0 Hz, 1H), 7.50 (t, *J* = 7.6 Hz, 1H), 7.29 (t, *J* = 7.4 Hz, 1H), 2.92 (s, 3H); ^{13}C{^{1}H} NMR (100 MHz, DMSO-d_6) δ 169.6, 168.6, 140.7, 140.2, 129.5, 127.5, 127.3, 127.2, 127.1, 126.2, 126.1, 124.4, 123.4 (d, *J* = 4.8 Hz), 121.4, 121.1 (d, *J* = 4.8 Hz), 121.0 (d, *J* = 4.9 Hz), 117.0, 112.8, 112.2, 23.8; HRMS (ESI) *m/z*: $[M + H]^+$ calculated for $C_{20}H_{12}F_3N_2O_2^+$, 369.0845; found, 369.0792.

4,6-Difluoro-2-methylbenzo[*a*]pyrrolo[3,4-*c*]carbazole-1,3(2*H*,8*H*)-dione (42ia): Green solid

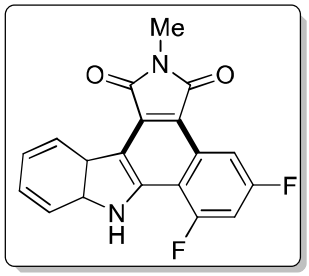

(72 mg, 98%); R_f = 0.2 (EtOAc/Hexane = 1: 4, *v/v*); mp = 320-322 °C; ^{1}H NMR (400 MHz, DMSO-d_6) δ 12.17 (s, 1H), 8.67 (d, *J* = 8.0 Hz, 1H), 8.12 (dd, *J* = 10.8, 2.4 Hz, 1H), 7.74 (d, *J* = 8.4 Hz, 1H), 7.58 – 7.50 (m, 2H), 7.32 (t, *J* = 7.4 Hz, 1H), 2.94 (s, 3H); ^{13}C{^{1}H} NMR (100 MHz, DMSO-d_6) δ 169.3, 168.3, 140.6, 136.4, 129.2, 127.1, 124.0, 121.5, 120.1, 116.1(d, *J* = 5.6 Hz), 113.0, 112.7, 109.6, 109.5, 104.8 (d, *J* = 4.2 Hz), 104.6, 103.4 (d, *J* = 5.8 Hz), 103.2, 23.8; HRMS (ESI) *m/z*: $[M + H]^+$ calculated for $C_{19}H_{11}F_2N_2O_2^+$, 337.0783; found, 337.0793.

2,11-Dimethylbenzo[*a*]pyrrolo[3,4-*c*]carbazole-1,3(2*H*,8*H*)-dione (42ja): Red solid (45 mg, 59%); R_f = 0.3 (EtOAc/Hexane = 1: 4, *v/v*); mp = 356-358 °C; ^{1}H NMR (400 MHz, DMSO-d_6) δ 12.71 (s, 1H), 8.89 – 8.87 (m, 1H), 8.58 – 8.56 (m, 2H), 7.78 – 7.72 (m, 2H), 7.57 (d, *J* = 6.8 Hz, 1H), 7.35 (d, *J* = 8.4, 1H), 3.07 (s, 3H), 2.51 (s, 3H); ^{13}C{^{1}H} NMR (100 MHz, DMSO-d_6) δ 170.4, 169.5, 140.9, 138.6, 129.9, 128.5, 128.3, 128.1, 127.9, 126.2, 125.2, 124.0, 123.1, 122.8, 121.8, 117.8, 112.1, 111.8, 23.9, 21.9; HRMS (ESI) *m/z*: $[M + H]^+$ calculated for $C_{20}H_{15}N_2O_2^+$, 315.1128; found, 315.1102.

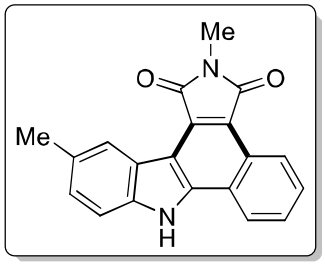

10-Chloro-2,5-dimethylbenzo[*a*]pyrrolo[3,4-*c*]carbazole-1,3(2*H*,8*H*)-dione (42ka): Red solid (36 mg, 50%); R_f = 0.4 (EtOAc/Hexane = 1: 6, *v/v*); mp = 319-321 °C; ^{1}H NMR (400 MHz, DMSO-d_6) δ 12.73 (s, 1H), 8.59 (d, *J* = 2.0 Hz, 1H), 8.44 (s, 1H), 8.28 (d, *J* = 8.4 Hz, 1H), 7.58 (d, *J* = 8.4 Hz, 1H), 7.50 (dd, *J* = 8.4, 1.6 Hz, 1H), 7.46 (dd, *J* = 8.4, 2.4 Hz, 1H), 2.97 (s, 3H), 2.51 (s, 3H); ^{13}C{^{1}H} NMR (100 MHz, DMSO-d_6) δ 170.1, 169.3, 141.3, 138.6, 138.6, 130.1, 127.7, 126.6, 126.5, 125.2, 124.1, 123.2, 123.0, 122.6, 120.8, 117.8, 113.6, 110.7, 23.8, 22.2; HRMS (ESI) *m/z*: $[M + H]^+$ calculated for $C_{20}H_{14}ClN_2O_2^+$, 349.0738; found, 349.0694.

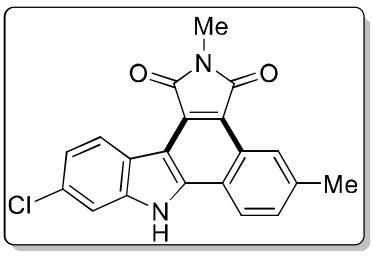

8-Methylnaphtho[1,2-*a*]pyrrolo[3,4-*c*]carbazole-7,9(8*H*,14*H*)-dione (42la): Red solid (57 mg, 79%); R_f = 0.3 (EtOAc/Hexane = 1: 3, *v/v*); mp = 303-305 °C; ^{1}H NMR (400 MHz, DMSO-d_6) δ 12.39 (s, 1H), 9.15 (d, *J* = 8.4 Hz, 1H), 9.01 (d, *J* = 8.0 Hz, 1H), 8.96 (d, *J* = 9.2 Hz, 1H), 8.12 (d, *J* = 6.8, 1H), 8.03 (d, *J* = 9.2 Hz, 1H), 7.94 – 7.89 (m, 2H), 7.81 (t, *J* = 8.0 Hz, 1H), 7.62 – 7.58 (m, 1H), 7.40 – 7.36 (m, 1H), 3.08 (s, 3H); ^{13}C{^{1}H} NMR (100 MHz, DMSO-d_6) δ 170.4, 169.1, 142.0, 140.1, 132.7, 129.8, 129.5, 128.6, 128.3, 127.8, 127.7, 126.8, 126.7, 126.4, 124.6, 122.4, 121.4, 120.8, 119.2, 118.3, 116.9, 113.1, 24.1; HRMS (ESI) *m/z*: $[M + H]^+$ calculated for $C_{23}H_{15}N_2O_2^+$, 351.1128; found, 351.1133.

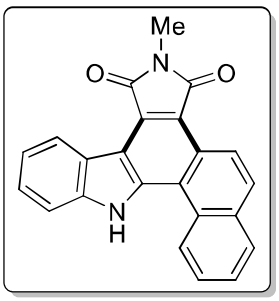

5-Methylpyrrolo[3,4-*c*]thieno[2,3-*a*]carbazole-4,6(5*H*,11*H*)-dione (42ma): Green solid (42 mg, 55%); R_f = 0.2 (EtOAc/Hexane = 1: 3, *v/v*); mp = 357-359 °C; ^{1}H NMR (400 MHz, DMSO-d_6) δ 12.70 (s, 1H), 8.87 (d, *J* = 8.0 Hz, 1H), 8.13 (d, *J* = 5.6 Hz, 1H), 8.00 (d, *J* = 5.6 Hz, 1H), 7.64 (d, *J* = 8.0 Hz, 1H), 7.55 (t, *J* = 7.4 Hz, 1H), 7.35 (t, *J* = 7.4 Hz, 1H), 3.10 (s, 3H); ^{13}C{^{1}H} NMR (100 MHz, DMSO-d_6) δ 169.8, 169.5, 141.1, 138.8, 133.1, 131.9, 127.6, 127.4, 125.1, 124.7, 122.2, 121.4, 121.1, 117.7, 113.8, 112.2, 24.0; HRMS (ESI) *m/z*: $[M + H]^+$ calculated for $C_{17}H_{11}N_2O_2S^+$, 307.0536; found, 307.0538.

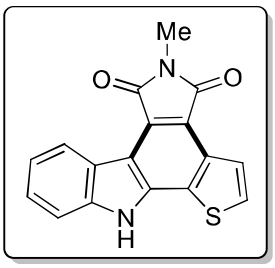

2-Ethylbenzo[*a*]pyrrolo[3,4-*c*]carbazole-1,3(2*H*,8*H*)-dione (42ab): Red solid (61 mg, 75%); R_f = 0.3 (EtOAc/Hexane = 1: 3, *v/v*); mp = 279-280 °C; ^{1}H NMR (400 MHz, DMSO-d_6) δ 12.85 (s, 1H), 8.93 – 8.91 (m, 1H), 8.85 (d, *J* = 8.0 Hz, 1H), 8.61 – 8.58 (m, 1H), 7.78 – 7.76 (m, 2H), 7.70 (d, *J* = 8.4 Hz, 1H), 7.55 (t, *J* = 7.6 Hz, 1H), 7.36 (t, *J* = 7.6 Hz, 1H), 3.68 (q, *J* = 7.2 Hz, 2H), 1.26 (t, *J* = 7.2 Hz, 3H); ^{13}C{^{1}H} NMR (100 MHz, DMSO-d_6) δ 170.2, 169.3, 140.8, 140.3, 128.7, 128.1, 128.0, 127.0, 126.3, 125.2, 124.4, 123.2, 122.8, 121.6, 121.2, 117.9, 112.3, 32.6, 14.5; HRMS (ESI) *m/z*: $[M + H]^+$ calculated for $C_{20}H_{15}N_2O_2^+$, 315.1128; found, 315.1106.

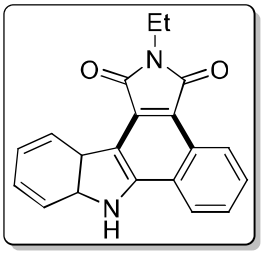

2-Benzylbenzo[*a*]pyrrolo[3,4-*c*]carbazole-1,3(2*H*,8*H*)-dione (42ac): Brown solid (56 mg, 58%); R_f = 0.4 (EtOAc/Hexane = 1: 4, *v/v*); mp = 270-272 °C; ^{1}H NMR (400 MHz, DMSO-d_6) δ 12.98 (s, 1H), 9.00 – 8.97 (m, 1H), 8.89 (d, *J* = 8.0 Hz, 1H), 8.69 – 8.67 (m, 1H), 7.86 – 7.80 (m, 2H), 7.75 (d, *J* = 8.0 Hz, 1H), 7.57 (t, *J* = 7.6 Hz, 1H), 7.43 – 7.41 (m, 2H), 7.36 (t, *J* = 7.8 Hz, 3H), 7.28 (t, *J* = 7.4 Hz, 1H), 4.88 (s, 2H); ^{13}C{^{1}H} NMR (100 MHz, DMSO-d_6) δ 170.2, 169.4, 141.1, 140.4, 137.7, 129.1, 128.9, 128.4, 128.1, 127.9, 127.8, 127.2, 126.5, 125.3, 124.4, 123.3, 123.0, 121.6, 121.3, 117.9, 112.4, 112.4, 41.2; HRMS (ESI) *m/z*: $[M + H]^+$ calculated for $C_{25}H_{17}N_2O_2^+$, 377.1285; found, 377.1249.

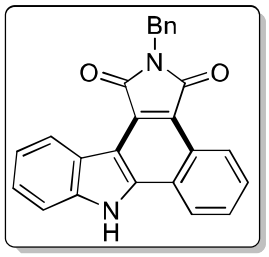

2-Phenylbenzo[*a*]pyrrolo[3,4-*c*]carbazole-1,3(2*H*,8*H*)-dione (42ad): Red solid (66 mg, 71%);

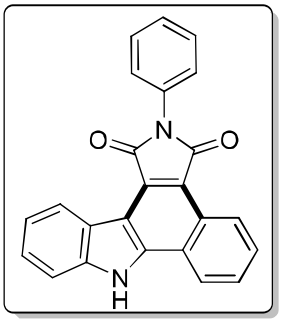

R_f = 0.5 (EtOAc/Hexane = 1: 4, *v/v*); mp = 254-256 °C; ^{1}H NMR (400 MHz, DMSO-d_6) δ 13.00 (s, 1H), 9.03 – 9.01 (m, 1H), 8.90 (d, *J* = 8.0 Hz, 1H), 8.70 – 8.68 (m, 1H), 7.87 – 7.83 (m, 2H), 7.75 (d, *J* = 8.0 Hz, 1H), 7.61 – 7.55 (m, 5H), 7.50 – 7.47 (m, 1H), 7.38 (t, *J* = 7.6 Hz, 1H); ^{13}C{^{1}H} NMR (100 MHz, DMSO-d_6) δ 169.4, 168.6, 141.1, 140.5, 132.7, 129.3, 128.9, 128.5, 128.2, 128.0, 127.1, 126.5, 125.4, 124.5, 123.3, 123.2, 121.7, 121.5, 117.7, 112.4, 112.4; HRMS (ESI) *m/z*: [M + H]$^+$ calculated for $C_{24}H_{15}N_2O_2^+$, 363.1128; found, 363.1109.

2-(*p*-Tolyl)benzo[*a*]pyrrolo[3,4-*c*]carbazole-1,3(2*H*,8*H*)-dione (42ae): Red solid (65 mg, 67%);

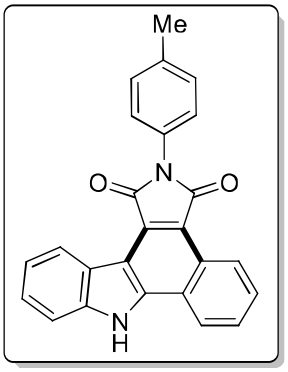

R_f = 0.3 (EtOAc/Hexane = 1: 4, *v/v*); mp = 289-291 °C; ^{1}H NMR (400 MHz, DMSO-d_6) δ 12.99 (s, 1H), 9.03 – 9.01 (m, 1H), 8.91 (d, *J* = 8.0 Hz, 1H), 8.71 – 8.69 (m, 1H), 7.87 – 7.81 (m, 2H), 7.75 (d, *J* = 8.0 Hz, 1H), 7.57 (t, *J* = 7.4 Hz, 1H), 7.45 (d, *J* = 8.4 Hz, 2H), 7.40 – 7.36 (m, 3H), 2.42 (s, 3H); ^{13}C{^{1}H} NMR (100 MHz, DMSO-d_6) δ 174.2, 173.4, 145.8, 145.1, 145.0, 142.4, 134.8, 134.5, 133.6, 133.1, 132.7, 132.6, 131.9, 131.2, 130.2, 129.2, 128.1, 127.8, 126.4, 126.1, 122.5, 117.1, 26.0 ; HRMS (ESI) *m/z*: [M + H]$^+$ calculated for $C_{25}H_{17}N_2O_2^+$, 377.1285; found, 377.1262.

2-(4-Methoxyphenyl)benzo[*a*]pyrrolo[3,4-*c*]carbazole-1,3(2*H*,8*H*)-dione (42af): Red solid (57

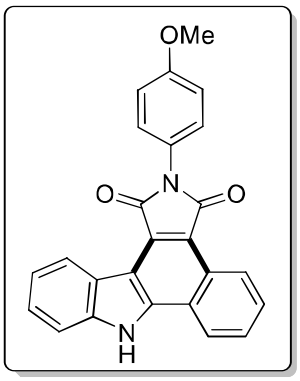

mg, 56%); R_f = 0.2 (EtOAc/Hexane = 1: 4, *v/v*); mp = 321-323 °C; ^{1}H NMR (400 MHz, DMSO-d_6) δ 13.00 (s, 1H), 9.04 – 9.02 (m, 1H), 8.92 (d, *J* = 8.0 Hz, 1H), 8.72 – 8.70 (m, 1H), 7.88 – 7.82 (m, 2H), 7.76 (d, *J* = 8.0 Hz, 1H), 7.58 (t, *J* = 7.2 Hz, 1H), 7.49 – 7.47 (m, 2H), 7.39 (t, *J* = 7.4 Hz, 1H), 7.14 – 7.12 (m, 2H), 3.86 (s, 3H); ^{13}C{^{1}H} NMR (100 MHz, DMSO-d_6) δ 169.7, 168.9, 159.2, 141.1, 140.5, 129.5, 128.9, 128.4, 128.1, 127.1, 126.6, 125.5, 125.3, 124.5, 123.4, 123.2, 121.7, 121.3, 117.8, 114.6, 112.4, 112.4, 55.9; HRMS (ESI) *m/z*: [M + H]$^+$ calculated for $C_{25}H_{17}N_2O_3^+$, 393.1234; found, 393.1203.

2-(4-Bromophenyl)benzo[*a*]pyrrolo[3,4-*c*]carbazole-1,3(2*H*,8*H*)-dione (42ag): Red solid (50 mg, 44%); R_f = 0.4 (EtOAc/Hexane = 1: 6, *v/v*); mp = 289-291 °C; ^{1}H NMR (400 MHz, DMSO-d_6) δ 13.02 (s, 1H), 9.03 – 9.00 (m, 1H), 8.90 (d, *J* = 8.0 Hz, 1H), 8.72 – 8.69 (m, 1H), 7.88 – 7.82 (m, 2H), 7.81 – 7.77 (m, 2H), 7.76 (d, *J* = 8.0 Hz, 1H), 7.60 – 7.55 (m, 3H), 7.41 – 7.37 (m, 1H); ^{13}C{^{1}H} NMR (100 MHz, DMSO-d_6) δ 173.8, 173.0, 145.9, 145.2, 137.0, 136.8, 134.7, 133.7, 133.3, 132.8, 131.9, 131.3, 130.2, 130.1, 129.3, 128.1, 127.9, 126.4, 126.1, 125.8, 122.5, 117.2; HRMS (ESI) *m/z*: $[M + H]^+$ calculated for $C_{24}H_{14}BrN_2O_2^+$, 441.0233; found, 441.0203.

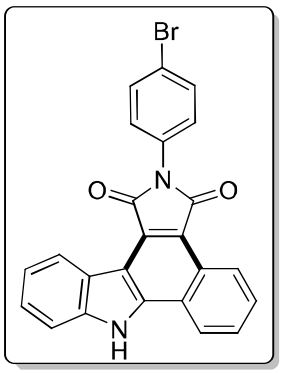

2-(4-Nitrophenyl)benzo[*a*]pyrrolo[3,4-*c*]carbazole-1,3(2*H*,8*H*)-dione (42ah): Yellow solid (50 mg, 48%); R_f = 0.2 (EtOAc/Hexane = 1: 3, *v/v*); mp = 296-298 °C; ^{1}H NMR (400 MHz, DMSO-d_6) δ 13.13 (s, 1H), 9.09 – 9.07 (m, 1H), 8.95 (d, *J* = 8.0 Hz, 1H), 8.78 – 8.76 (m, 1H), 8.46 (d, *J* = 9.2 Hz, 2H), 7.95 (d, *J* = 9.2 Hz, 2H), 7.92 – 7.88 (m, 2H), 7.80 (d, *J* = 8.2 Hz, 1H), 7.61 (t, *J* = 7.4 Hz, 1H), 7.43 (t, *J* = 7.6 Hz, 1H); ^{13}C{^{1}H} NMR (100 MHz, DMSO-d_6) δ 168.7, 168.0, 146.2, 141.4, 140.6, 138.7, 138.7, 129.2, 128.8, 128.8, 128.0, 127.3, 126.6, 125.5, 124.6, 124.5, 123.5, 121.7, 121.5, 117.8, 117.5, 112.5; HRMS (ESI) *m/z*: $[M + H + Na]^+$ calculated for $C_{24}H_{14}N_3NaO_4^+$, 431.0877; found, 431.0891.

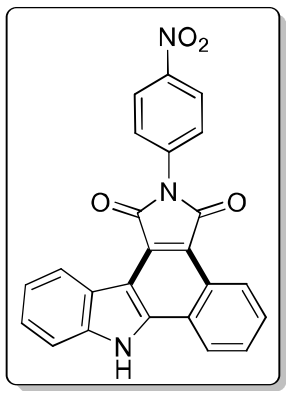

2-(Naphthalen-1-yl)benzo[*a*]pyrrolo[3,4-*c*]carbazole-1,3(2*H*,8*H*)-dione (42ai): Green solid (46 mg, 43%); R_f = 0.4 (EtOAc/Hexane = 1: 6, *v/v*); mp = 159-161 °C; ^{1}H NMR (400 MHz, DMSO-d_6) δ 13.09 (s, 1H), 9.06 (d, *J* = 7.6 Hz, 1H), 8.90 (d, *J* = 8.0 Hz, 1H), 8.78 (d, *J* = 8.8 Hz, 1H), 8.17 – 8.11 (m, 2H), 7.94 – 7.85 (m, 3H), 7.81 – 7.71 (m, 3H), 7.65 – 7.54 (m, 3H), 7.38 (t, *J* = 7.6 Hz, 1H); ^{13}C{^{1}H} NMR (100 MHz, DMSO-d_6) δ 170.1, 169.3, 141.3, 140.5, 134.3, 131.2, 129.8, 129.4, 129.0, 128.8, 128.6, 128.4, 128.3, 127.6, 127.2, 127.0, 126.8, 126.2, 125.6, 124.5, 123.5, 123.4, 123.3, 121.8, 121.4, 118.2, 112.7, 112.5; HRMS (ESI) *m/z*: $[M + H]^+$ calculated for $C_{28}H_{17}N_2O_2^+$, 413.1285; found, 413.1255.

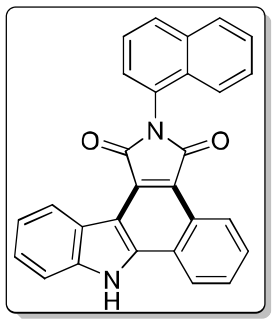

Benzo[*a*]pyrrolo[3,4-*c*]carbazole-1,3(2*H*,8*H*)-dione (42aj): Red solid (45 mg, 61%); R_f = 0.2 (EtOAc/Hexane = 1: 3, *v/v*); mp = 324-326 °C; ^{1}H NMR (400 MHz, DMSO-d_6) δ 12.97 (s, 1H), 11.16 (s, 1H), 9.03 – 9.01 (m, 1H), 8.92 (d, *J* = 8.0 Hz, 1H), 8.74 – 8.70 (m, 1H), 7.89 – 7.80 (m, 2H), 7.76 (d, *J* = 8.0 Hz, 1H), 7.60 – 7.55 (m, 1H), 7.42 – 7.38 (m, 1H); ^{13}C{^{1}H} NMR (100 MHz, DMSO-d_6) δ 172.0, 171.0, 140.9, 140.4, 129.1, 128.7, 128.3, 127.0, 126.5, 125.4, 124.5, 123.3, 123.2, 121.8, 121.2, 119.0, 112.3; HRMS (ESI) *m/z*: $[M + Na]^+$ calculated for $C_{18}H_{10}N_2NaO_2^+$, 309.0634; found, 309.0634.

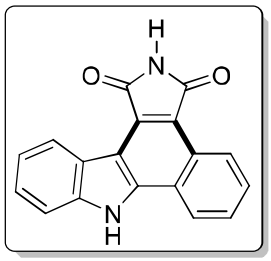

5-Methylpyrazolo[1',5':1,6]pyrrolo[3',4':4,5]pyrido[2,3-*b*]indole-4,6(5*H*,11*H*)-dione (44aa): Red solid (52 mg, 66%); R_f = 0.2 (EtOAc/Hexane = 1: 3, *v/v*); mp = 333-335 °C; ^{1}H NMR (400 MHz, DMSO-d_6) δ 13.67 (s, 1H), 8.57 (d, *J* = 8.0 Hz, 1H), 8.44 (s, 1H), 7.66 (d, *J* = 8.0 Hz, 1H), 7.49 (t, *J* = 7.6 Hz, 1H), 7.39 (t, *J* = 7.6 Hz, 1H), 7.10 (s, 1H), 3.11 (s, 3H); ^{13}C{^{1}H} NMR (100 MHz, DMSO-d_6) δ 168.7, 168.1, 145.2, 137.5, 133.7, 128.0, 126.2, 123.2, 122.6, 121.3, 113.1, 100.2, 100.0, 98.3, 24.3; HRMS (ESI) *m/z*: $[M + H]^+$ calculated for $C_{16}H_{11}N_4O_2^+$, 291.0877; found, 291.0872.

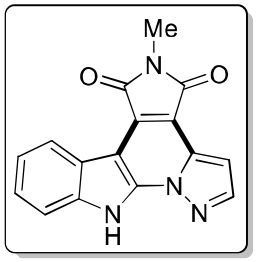

5,8-Dimethylpyrazolo[1',5':1,6]pyrrolo[3',4':4,5]pyrido[2,3-*b*]indole-4,6(5*H*,11*H*)-dione (44ba): Orange solid (49 mg, 64%); R_f = 0.2 (EtOAc/Hexane = 3: 7, *v/v*); mp = 345-347 °C; ^{1}H NMR (400 MHz, DMSO-d_6) δ 13.53 (s, 1H), 8.42 – 8.32 (m, 2H), 7.53 (d, *J* = 8.0 Hz, 1H), 7.30 (d, *J* = 8.4 Hz, 1H), 7.08 (s, 1H), 3.10 (s, 3H), 2.51 (s, 3H); ^{13}C{^{1}H} NMR (100 MHz, DMSO-d_6) δ 168.7, 168.2, 153.3, 146.5, 145.2, 135.7, 133.7, 131.5, 130.7, 128.1, 127.5, 123.0, 121.5, 112.8, 98.3, 24.2, 21.8; HRMS (ESI) *m/z*: $[M + H]^+$ calculated for $C_{17}H_{13}N_4O_2^+$, 305.1033; found, 305.1012.

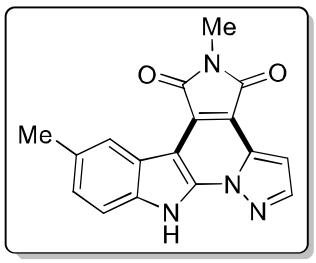

8-Methoxy-5-methylpyrazolo[1',5':1,6]pyrrolo[3',4':4,5]pyrido[2,3-*b*]indole-4,6(5*H*,11*H*)-dione (44da): 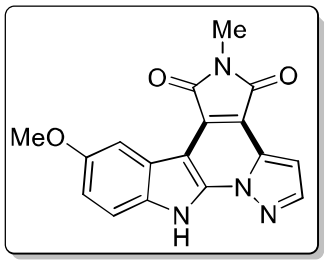

Orange solid (41 mg, 55%); R_f = 0.3 (EtOAc/Hexane = 3: 7, *v/v*); mp = 343-345 °C; ^{1}H NMR (400 MHz, DMSO-d_6) δ 13.39 (s, 1H), 8.36 (d, *J* = 2.0 Hz, 1H), 7.97 (s, 1H), 7.48 (d, *J* = 8.8 Hz, 1H), 7.05 (dd, *J* = 8.8, 2.4 Hz, 1H), 7.00 – 6.99 (m, 1H), 3.84 (s, 3H), 3.05 (s, 3H); ^{13}C{^{1}H} NMR (100 MHz, DMSO-d_6) δ 168.6, 168.0, 155.5, 144.9, 139.4, 133.5, 131.9, 127.9, 121.8, 115.0, 113.8, 111.0, 105.6, 100.2, 98.2, 55.8, 24.1; HRMS (ESI) *m/z*: $[M + H]^+$ calculated for $C_{17}H_{13}N_4O_3^+$, 321.0982; found, 321.0975.

5-Ethylpyrazolo[1',5':1,6]pyrrolo[3',4':4,5]pyrido[2,3-*b*]indole-4,6(5*H*,11*H*)-dione (44ab): 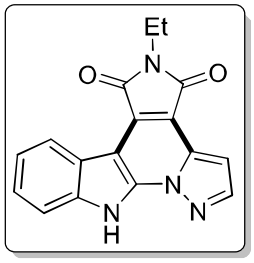

Orange solid (51 mg, 61%); R_f = 0.3 (EtOAc/Hexane = 1: 3, *v/v*); ^{1}H NMR (400 MHz, DMSO-d_6) δ 13.66 (s, 1H), 8.57 (d, *J* = 8.0 Hz, 1H), 8.44 (d, *J* = 2.0 Hz, 1H), 7.65 (d, *J* = 8.0 Hz, 1H), 7.51 – 7.47 (m, 1H), 7.41 – 7.37 (m, 1H), 7.10 (d, *J* = 2.0 Hz, 1H), 3.68 (q, *J* = 7.2 Hz, 2H), 1.25 (t, *J* = 7.2 Hz, 3H); ^{13}C{^{1}H} NMR (100 MHz, DMSO-d_6) δ 168.4, 167.9, 145.3, 139.4, 137.5, 133.8, 128.0, 126.3, 123.2, 122.6, 121.3, 113.2, 111.7, 100.2, 98.4, 32.9, 14.4; HRMS (ESI) *m/z*: $[M + H]^+$ calculated for $C_{17}H_{13}N_4O_2^+$, 305.1033; found, 305.1003.

5-Benzylpyrazolo[1',5':1,6]pyrrolo[3',4':4,5]pyrido[2,3-*b*]indole-4,6(5*H*,11*H*)-dione (44ac): 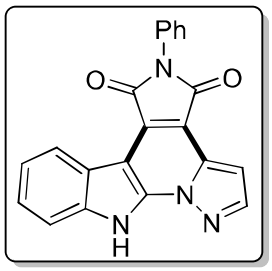

Orange solid (51 mg, 51%); R_f = 0.3 (EtOAc/Hexane = 1: 3, *v/v*); mp = 260-262 °C; ^{1}H NMR (400 MHz, DMSO-d_6) δ 13.72 (s, 1H), 8.56 (d, *J* = 7.6 Hz, 1H), 8.44 (d, *J* = 2.4 Hz, 1H), 7.65 (d, *J* = 8.0 Hz, 1H), 7.50 – 7.46 (m, 1H), 7.42 – 7.34 (m, 5H), 7.31 – 7.26 (m, 1H), 7.10 (d, *J* = 2.3 Hz, 1H), 4.85 (s, 2H); ^{13}C{^{1}H} NMR (100 MHz, DMSO-d_6) δ 168.5, 167.8, 145.2, 138.0, 137.4, 133.8, 129.1, 128.8, 127.9, 127.9, 126.2, 123.2, 122.5, 121.4, 113.4, 104.5, 100.4, 98.4, 41.4; HRMS (ESI) *m/z*: $[M + H]^+$ calculated for $C_{22}H_{15}N_4O_2^+$, 367.1190; found, 367.1161.

5-Phenylpyrazolo[1',5':1,6]pyrrolo[3',4':4,5]pyrido[2,3-*b*]indole-4,6(5*H*,11*H*)-dione (44ad):

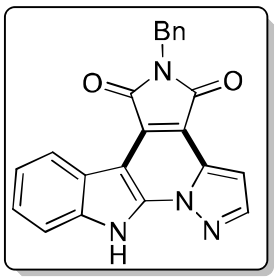

Orange solid (47 mg, 49%); R_f = 0.4 (EtOAc/Hexane = 1: 4, *v/v*); mp = 364-366 °C; ^{1}H NMR (400 MHz, DMSO-d_6) δ 13.74 (s, 1H), 8.58 (d, *J* = 8.0 Hz, 1H), 8.48 (d, *J* = 2.4 Hz, 1H), 7.67 (d, *J* = 8.0 Hz, 1H), 7.61 – 7.55 (m, 4H), 7.52 – 7.46 (m, 2H), 7.38 (t, *J* = 7.6 Hz, 1H), 7.16 (d, *J* = 2.34Hz, 1H); ^{13}C{^{1}H} NMR (100 MHz, DMSO-d_6) δ 167.6, 167.0, 145.4, 139.6, 137.5, 133.9, 132.5, 129.4, 128.3, 127.9, 127.8, 126.3, 123.3, 122.7, 121.3, 113.2, 111.5, 100.3, 98.8; HRMS (ESI) *m/z*: [M + H]$^+$ calculated for $C_{21}H_{13}N_4O_2^+$, 353.1033; found, 353.1038.

Pyrazolo[1',5':1,6]pyrrolo[3',4':4,5]pyrido[2,3-*b*]indole-4,6(5*H*,11*H*)-dione (44aj): Red solid

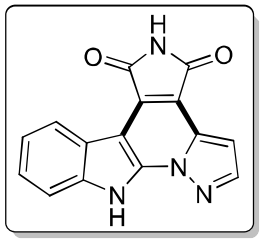

(35 mg, 47%); R_f = 0.3 (EtOAc/Hexane = 2: 3, *v/v*); mp = 327-329 °C; ^{1}H NMR (400 MHz, DMSO-d_6) δ 13.69 (s, 1H), 11.28 (s, 1H), 8.61 (d, *J* = 7.6 Hz, 1H), 8.46 (s, 1H), 7.68 (d, *J* = 8.0 Hz, 1H), 7.50 (t, *J* = 7.4 Hz, 1H), 7.41 (t, *J* = 7.0 Hz, 1H), 7.12 (s, 1H); ^{13}C{^{1}H} NMR (100 MHz, DMSO-d_6) δ 170.1, 169.5, 145.1, 139.6, 137.6, 133.8, 128.9, 126.1, 123.3, 122.5, 121.5, 113.2, 112.6, 100.1, 98.5; HRMS (ESI) *m/z*: [M + H]$^+$ calculated for $C_{15}H_9N_4O_2^+$, 277.0720; found, 277.0712.

7-Methyl-5,13-dihydro-6*H*-indolo[3,2-*a*]pyrrolo[3,4-*c*]carbazole-6,8(7*H*)-dione (44da):

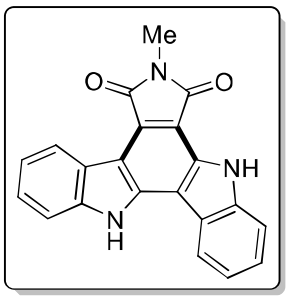

Yellow solid (50 mg, 68%); R_f = 0.4 (EtOAc/Hexane = 1: 3, *v/v*); mp = 346-348 °C; ^{1}H NMR (400 MHz, DMSO-d_6) δ 12.29 (s, 1H), 12.16 (s, 1H), 8.94 (d, *J* = 8.0 Hz, 1H), 8.77 (d, *J* = 8.0 Hz, 1H), 7.76 (d, *J* = 8.0 Hz, 1H), 7.73 (d, *J* = 8.0 Hz, 1H), 7.54 (q, *J* = 7.4 Hz, 2H), 7.41 (t, *J* = 7.6 Hz, 1H), 7.34 (t, *J* = 7.4 Hz, 1H), 3.16 (s, 3H); ^{13}C{^{1}H} NMR (100 MHz, DMSO-d_6) δ 170.1, 169.4, 141.7, 141.6, 138.6, 133.0, 126.8, 126.7, 124.2, 124.1, 122.3, 121.6, 120.8, 120.6, 120.6, 112.7, 112.5, 112.0, 111.2, 106.9, 24.1; HRMS (ESI) *m/z*: [M + H]$^+$ calculated for $C_{21}H_{14}N_3O_2^+$, 340.1081; found, 340.1102.

5,13-Dihydro-6*H*-indolo[3,2-*a*]pyrrolo[3,4-*c*]carbazole-6,8(7*H*)-dione (44dj): Yellow solid

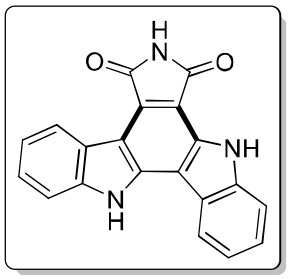

(39 mg, 56%); R_f = 0.3 (EtOAc/Hexane = 1: 3, *v/v*); mp = >350 °C; ^{1}H NMR (400 MHz, DMSO-d_6) δ 12.32 (s, 1H), 12.17 (s, 1H), 11.04 (s, 1H), 8.94 (d, *J* = 7.6 Hz, 1H), 8.78 (d, *J* = 7.6 Hz, 1H), 7.75 (t, *J* = 9.6 Hz, 2H), 7.54 (q, *J* = 7.2 Hz, 2H), 7.43 – 7.33 (m, 2H); ^{13}C{^{1}H} NMR (100 MHz, DMSO-d_6) δ 171.5, 170.7, 144.1, 141.6, 138.7, 132.9, 126.7, 126.7, 125.2, 124.2, 122.3, 121.7, 120.8, 120.6, 120.6, 112.7, 112.3, 112.0, 111.3, 107.9; HRMS (ESI) *m/z*: $[M + H]^+$ calculated for $C_{20}H_{12}N_3O_2^+$, 326.0924; found, 326.0882

1'-Methyl-11-phenylspiro[isoindolo[2,1-*a*]indole-6,3'-pyrrolidine]-2',5'-dione (46aa): Off

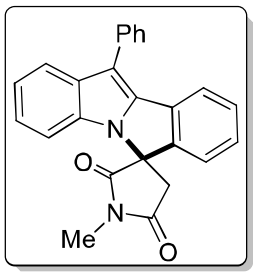

white solid (64 mg, 91%); R_f = 0.5 (EtOAc/Hexane = 1: 3, *v/v*); mp = 190-192 °C; ^{1}H NMR (400 MHz, DMSO-d_6) δ 7.77 – 7.69 (m, 5H), 7.61 (t, *J* = 7.6 Hz, 2H), 7.49 (t, *J* = 7.2 Hz, 1H), 7.46 – 7.42 (m, 2H), 7.33 (d, *J* = 8.0 Hz, 1H), 7.25 (t, *J* = 7.4 Hz, 1H), 7.18 (t, *J* = 7.2 Hz,1H), 3.70 (d, *J* = 18.4 Hz, 1H), 3.51 (d, *J* = 18.8 Hz, 1H), 3.15 (s, 3H); ^{13}C{^{1}H} NMR (100 MHz, DMSO-d_6) δ 174.4, 173.9, 145.7, 138.7, 133.8, 132.4, 131.8, 131.6, 130.3, 129.5, 129.3, 129.1, 127.4, 123.7, 123.3, 121.4, 120.8, 120.7, 110.4, 110.1, 68.1, 40.1, 26.1; HRMS (ESI) *m/z*: $[M + HCOO]^-$ calculated for $C_{25}H_{19}N_2O_4^-$, 423.1350; found, 423.1339.

1',2-Dimethyl-11-phenylspiro[isoindolo[2,1-*a*]indole-6,3'-pyrrolidine]-2',5'-dione (46ba):

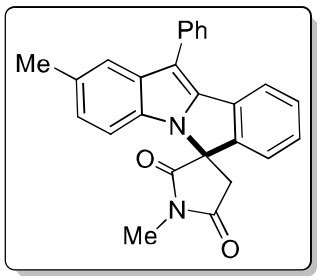

Off white solid (55 mg, 80%); R_f = 0.4 (EtOAc/Hexane = 1: 3, *v/v*); mp = 197-199 °C; ^{1}H NMR (400 MHz, DMSO-d_6) δ 7.74 – 7.67 (m, 4H), 7.60 (t, *J* = 7.4 Hz, 2H), 7.52 (s, 1H), 7.52 – 7.40 (m, 3H), 7.21 (d, *J* = 8.4 Hz, 1H), 7.07 (d, *J* = 8.4 Hz, 1H), 3.66 (d, *J* = 18.4 Hz, 1H), 3.50 (d, *J* = 18.4 Hz, 1H), 3.14 (s, 3H), 2.40 (s, 3H); ^{13}C{^{1}H} NMR (100 MHz, DMSO-d_6) δ 174.4, 173.9, 145.6, 138.8, 133.9, 132.1, 131.7, 130.8, 130.3, 129.5, 129.3, 129.0, 127.3, 125.2, 123.2, 120.7, 120.3, 110.0, 109.8, 68.0, 40.1, 26.1, 21.7; HRMS (ESI) *m/z*: $[M + H]^+$ calculated for $C_{26}H_{21}N_2O_2^+$, 393.1598; found, 393.1567.

2-Methoxy-1'-methyl-11-phenylspiro[isoindolo[2,1-*a*]indole-6,3'-pyrrolidine]-2',5'-dione

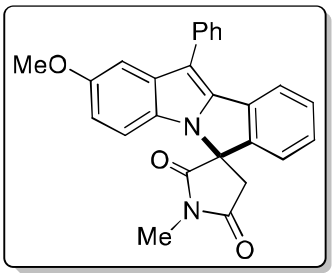

(46ca): Off white solid (61 mg, 90%); R_f = 0.5 (EtOAc/Hexane = 1: 3, *v/v*); mp = 189-191 °C; ^{1}H NMR (400 MHz, DMSO-d_6) δ 7.72 – 7.61 (m, 6H), 7.44 (s, 3H), 7.25 – 7.18 (m, 2H), 6.89 (s, 1H), 3.78 (s, 3H), 3.66 (d, *J* = 17.2 Hz, 1H), 3.49 (d, *J* = 20.0 Hz, 1H), 3.14 (s, 3H); ^{13}C{^{1}H} NMR (100 MHz, DMSO-d_6) δ 174.4, 173.9, 155.3, 145.7, 139.4, 134.0, 132.4, 131.8, 130.2, 129.6, 129.2, 128.9, 127.6, 127.3, 123.2, 120.6, 113.5, 110.9, 110.2, 102.6, 68.1, 55.9, 40.1, 26.1; HRMS (ESI) *m/z*: [M + H]$^+$ calculated for $C_{26}H_{21}N_2O_3^+$, 409.1547; found, 409.1592.

2-Bromo-1'-methyl-11-phenylspiro[isoindolo[2,1-*a*]indole-6,3'-pyrrolidine]-2',5'-dione

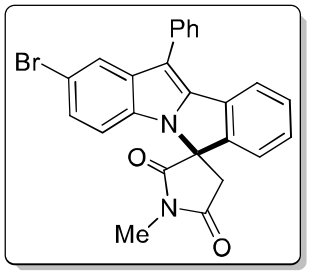

(46da): Off white solid (45 mg, 69%); R_f = 0.2 (EtOAc/Hexane = 1: 3, *v/v*); mp = 218-220 °C; ^{1}H NMR (400 MHz, DMSO-d_6) δ 7.81 (s, 1H), 7.76 – 7.67 (m, 4H), 7.62 (t, *J* = 7.4 Hz, 2H), 7.52 – 7.41 (m, 4H), 7.37 (d, *J* = 8.4 Hz, 1H), 3.72 (d, *J* = 18.8 Hz, 1H), 3.50 (d, *J* = 18.4 Hz, 1H), 3.14 (s, 3H); ^{13}C{^{1}H} NMR (100 MHz, DMSO-d_6) δ 174.1, 173.7, 145.8, 140.2, 133.5, 133.0, 131.2, 131.0, 130.4, 129.7, 129.6, 129.3, 127.7, 126.1, 123.2, 122.6, 121.1, 114.0, 112.3, 109.9, 68.3, 40.1, 26.2; HRMS (ESI) *m/z*: [M + H]$^+$ calculated for $C_{25}H_{18}BrN_2O_2^+$, 457.0546; found, 457.0519.

1'-Ethyl-11-phenylspiro[isoindolo[2,1-*a*]indole-6,3'-pyrrolidine]-2',5'-dione (46ab): Off white solid (65 mg, 90%); R_f = 0.3 (EtOAc/Hexane = 1: 3, *v/v*); mp = 201-203 °C; ^{1}H NMR (400 MHz, DMSO-d_6) δ 7.73 – 7.61 (m, 7H), 7.50 – 7.45 (m, 3H), 7.27 – 7.19 (m, 3H), 3.76 – 3.71 (m, 3H), 3.55 (d, *J* = 18.4 Hz, 1H), 1.24 (s, 3H); ^{13}C{^{1}H} NMR (100 MHz, DMSO-d_6) δ 178.8, 178.4, 150.3, 143.5, 138.5, 137.2, 136.6, 136.4, 135.1, 135.1, 134.3, 134.0, 134.0, 132.1, 128.5, 127.8, 126.1, 125.6, 115.2, 114.7, 72.7, 39.6, 18.0; HRMS (ESI) *m/z*: [M + H]$^+$ calculated for. $C_{26}H_{21}N_2O_2^+$, 393.1598; found, 393.1571

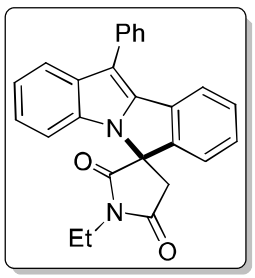

1'-Benzyl-11-phenylspiro[isoindolo[2,1-*a*]indole-6,3'-pyrrolidine]-2',5'-dione (46ac): Off white solid (65 mg, 77%); R_f = 0.3 (EtOAc/Hexane = 1: 3, *v/v*); mp = 193-195 °C; ^{1}H NMR (400 MHz, DMSO-d_6) δ 7.75 (d, *J* = 7.6 Hz, 2H), 7.71 (d, *J* = 7.2 Hz, 2H), 7.62 – 7.56 (m, 3H), 7.50 – 7.46 (m, 2H), 7.43 – 7.36 (m, 6H), 7.14 (t, *J* = 7.6 Hz, 1H), 7.07 (t, *J* = 7.2 Hz, 1H), 6.98 (d, *J* = 8.0 Hz, 1H), 4.84 (s, 2H), 3.78 (d, *J* = 18.8 Hz, 1H), 3.64 (d, *J* = 18.8 Hz, 1H); ^{13}C{^{1}H} NMR (100 MHz, DMSO-d_6) δ 174.2, 173.7, 145.4, 138.7, 136.0, 133.7, 132.3, 131.8, 131.7, 130.4, 129.5, 129.3, 129.1, 129.1, 128.8, 128.5, 127.4, 123.4, 123.2, 121.3, 120.9, 120.7, 110.4, 109.9, 68.0, 43.4, 39.5; HRMS (ESI) *m/z*: $[M + H]^+$ calculated for $C_{31}H_{23}N_2O_2^+$, 455.1754; found, 455.1727.

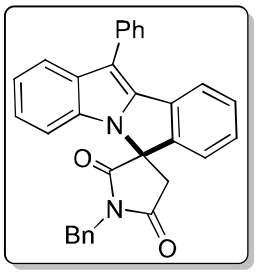

1',11-Diphenylspiro[isoindolo[2,1-*a*]indole-6,3'-pyrrolidine]-2',5'-dione (46ad): Off white solid (60 mg, 73%); R_f = 0.4 (EtOAc/Hexane = 1: 3, *v/v*); mp = 197-199 °C; ^{1}H NMR (400 MHz, DMSO-d_6) δ 7.92 (d, *J* = 6.4 Hz, 1H), 7.80 – 7.74 (m, 4H), 7.64 – 7.48 (m, 10H), 7.45 (t, *J* = 7.4 Hz, 1H), 7.33 (t, *J* = 7.6 Hz, 1H), 7.22 (t, *J* = 7.6 Hz, 1H), 3.97 (d, *J* = 18.8 Hz, 1H), 3.73 (d, *J* = 18.4 Hz, 1H); ^{13}C{^{1}H}MR (100 MHz, DMSO-d_6) δ 173.7, 172.9, 145.5, 138.8, 133.7, 132.6, 132.3, 131.9, 131.6, 130.5, 129.7, 129.6, 129.6, 129.3, 129.3, 127.6, 127.4, 123.9, 123.3, 121.5, 120.9, 120.8, 110.6, 110.2, 68.3; HRMS (ESI) *m/z*: $[M + H]^+$ calculated for $C_{30}H_{21}N_2O_2^+$, 441.1598; found, 441.1560.

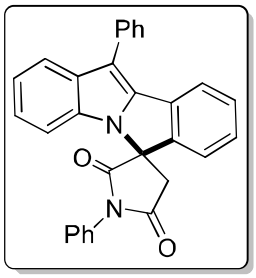

3.3B.4.3 X-ray Crystallographic Analysis of 42ab

Single crystals of **42ab** [$C_{22}H_{20}N_2O_3S$] were grown from DMSO solution as yellow colour blocks. The single crystal XRD data collection and data reduction were performed using CrysAlis PRO on a single crystal Rigaku Oxford XtaLab Pro Kappa dual home/near diffractometer. The crystal was kept at 93(2) K during data collection using CuKα (λ = 1.54184 Å). Using Olex2[77], the structure was solved with the ShelXT[78] structure solution program using Intrinsic Phasing and refined with the ShelXL[79] refinement package using Least Squares minimization.

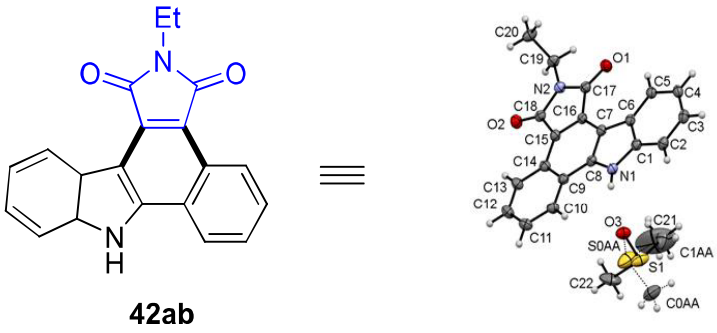

Figure 3.3B.11 ORTEP diagram of **42ab** (CCDC No 2024848). The thermal ellipsoids are drawn at 50% probability level.

Table 3.3B.6 Crystal data and structure refinement for **42ab (exp-637-VNS-982).**

Identification code	Exp-637-VNS-982
Empirical formula	$C_{22}H_{20}N_2O_3S$
Formula weight	392.46
Temperature/K	93(2)
Crystal system	triclinic
Space group	P-1
a/Å	8.3060(2)
b/Å	11.1596(3)
c/Å	11.9556(3)
α/°	63.393(3)
β/°	72.607(2)
γ/°	87.570(2)
Volume/Å^3	940.07(5)
Z	2
ρ_{calc}g/cm^3	1.386
μ/mm^{-1}	1.749
F(000)	412.0
Crystal size/mm^3	0.1 × 0.08 × 0.04
Radiation	CuKα (λ = 1.54184)
2Θ range for data collection/°	8.712 to 159.174
Index ranges	-10 ≤ h ≤ 10, -14 ≤ k ≤ 13, -15 ≤ l ≤ 14
Reflections collected	10170
Independent reflections	3962 [R_{int} = 0.0287, R_{sigma} = 0.0371]
Data/restraints/parameters	3962/0/285
Goodness-of-fit on F^2	1.098
Final R indexes [I>=2σ (I)]	R_1 = 0.0450, wR_2 = 0.1192
Final R indexes [all data]	R_1 = 0.0482, wR_2 = 0.1216
Largest diff. peak/hole / e Å^{-3}	0.49/-0.31

3.3B.5 REFERENCES

1. Colby, D. A.; Tsai, A. S.; Bergman, R. G.; Ellman, J. A., *Accounts of Chemical Research* **2012,** *45*, 814-825.
2. Gao, K.; Yoshikai, N., *Accounts of Chemical Research* **2014,** *47*, 1208-1219.
3. Gensch, T.; Hopkinson, M.; Glorius, F.; Wencel-Delord, J., *Chemical Society Reviews* **2016,** *45*, 2900-2936.
4. Gandeepan, P.; Müller, T.; Zell, D.; Cera, G.; Warratz, S.; Ackermann, L., *Chemical Reviews* **2018,** *119*, 2192-2452.
5. Rej, S.; Ano, Y.; Chatani, N., *Chemical Reviews* **2020,** *120*, 1788-1887.
6. Nakamura, I.; Yamamoto, Y., *Chemical Reviews* **2004,** *104*, 2127-2198.
7. Wang, H.; Xu, H.; Li, B.; Wang, B., *Organic Letters* **2018,** *20*, 5640-5643.
8. Li, C.; Qin, H. L., *Organic Letters* **2019,** *21*, 4495-4499.
9. Zeni, G.; Larock, R. C., *Chemical Reviews* **2006,** *106*, 4644-4680.
10. Xu, L.; Li, T.; Wang, L.; Cui, X., *The Journal of Organic Chemistry* **2018,** *84*, 560-567.
11. Yang, Z.; Song, Z.; Jie, L.; Wang, L.; Cui, X., *Chemical Communications* **2019,** *55*, 6094-6097.
12. Kumar, S. V.; Banerjee, S.; Punniyamurthy, T., *Organic Chemistry Frontiers* **2020,** *7*, 1527-1569.
13. Gulías, M.; Mascareñas, J. L., *Angewandte Chemie International Edition* **2016,** *55*, 11000-11019.
14. Zhu, C.; Wang, C. Q.; Feng, C., *Tetrahedron Letters* **2018,** *59*, 430-437.
15. Kurihara, T.; Kojima, M.; Yoshino, T.; Matsunaga, S., *Asian Journal of Organic Chemistry* **2020,** *9*, 368-371.
16. Huang, H.; Ji, X.; Wu, W.; Jiang, H., *Chemical Society Reviews* **2015,** *44*, 1155-1171.
17. Li, S. S.; Qin, L.; Dong, L., *Organic & Biomolecular Chemistry* **2016,** *14*, 4554-4570.
18. Satoh, T.; Miura, M., *Chemistry–A European Journal* **2010,** *16*, 11212-11222.
19. Bin, J. W.; Wong, I. L.; Hu, X.; Yu, Z. X.; Xing, L. F.; Jiang, T.; Chow, L. M.; Biao, W. S., *Journal of Medicinal Chemistry* **2013,** *56*, 9057-9070.
20. Miura, W.; Hirano, K.; Miura, M., *Organic Letters* **2015,** *17*, 4034-4037.
21. Zhao, H.; Shao, X.; Wang, T.; Zhai, S.; Qiu, S.; Tao, C.; Wang, H.; Zhai, H., *Chemical Communications* **2018,** *54*, 4927-4930.

22. Yuan, Y. C.; Goujon, M.; Bruneau, C.; Roisnel, T.; Gramage-Doria, R., *The Journal of Organic Chemistry* **2019,** *84*, 16183-16191.
23. Manoharan, R.; Jeganmohan, M., *Asian Journal of Organic Chemistry* **2019,** *8*, 1949-1969.
24. Zhu, C.; Luan, J.; Fang, J.; Zhao, X.; Wu, X.; Li, Y.; Luo, Y., *Organic Letters* **2018,** *20*, 5960-5963.
25. Han, S. H.; Mishra, N. K.; Jeon, M.; Kim, S.; Kim, H. S.; Jung, S. Y.; Jung, Y. H.; Ku, J. M.; Kim, I. S., *Advanced Synthesis & Catalysis* **2017,** *359*, 3900-3904.
26. Ramesh, B.; Tamizmani, M.; Jeganmohan, M., *The Journal of Organic Chemistry* **2019,** *84*, 4058-4071.
27. Sharma, S.; Oh, Y.; Mishra, N. K.; De, U.; Jo, H.; Sachan, R.; Kim, H. S.; Jung, Y. H.; Kim, I. S., *The Journal of Organic Chemistry* **2017,** *82*, 3359-3367.
28. Guo, C.; Li, B.; Liu, H.; Zhang, X.; Zhang, X.; Fan, X., *Organic Letters* **2019,** *21*, 7189-7193.
29. Li, H.; Zhang, S.; Feng, X.; Yu, X.; Yamamoto, Y.; Bao, M., *Organic Letters* **2019,** *21*, 8563-8567.
30. Devkota, S.; Lee, H. J.; Kim, S. H.; Lee, Y. R., *Advanced Synthesis & Catalysis* **2019,** *361*, 5587-5595.
31. Dhuguru, J.; Skouta, R., *Molecules* **2020,** *25*, 1615.
32. Thanikachalam, P. V.; Maurya, R. K.; Garg, V.; Monga, V., *European Journal of Medicinal Chemistry* **2019,** *180*, 562-612.
33. Sinha, A. K.; Equbal, D.; Uttam, M. R., *Chemistry of Heterocyclic Compounds* **2018,** *54*, 292-301.
34. Berlinck, R. G.; Britton, R.; Piers, E.; Lim, L.; Roberge, M.; Moreira da Rocha, R.; Andersen, R. J., *The Journal of Organic Chemistry* **1998,** *63*, 9850-9856.
35. Roberge, M.; Berlinck, R. G.; Xu, L.; Anderson, H. J.; Lim, L. Y.; Curman, D.; Stringer, C. M.; Friend, S. H.; Davies, P.; Vincent, I., *Cancer Research* **1998,** *58*, 5701-5706.
36. Sherikar, M. S.; Kapanaiah, R.; Lanke, V.; Prabhu, K. R., *Chemical Communications* **2018,** *54*, 11200-11203.
37. Lanke, V.; Bettadapur, K. R.; Prabhu, K. R., *Organic Letters* **2015,** *17*, 4662-4665.
38. Banjare, S. K.; Nanda, T.; Ravikumar, P., *Organic Letters* **2019,** *21*, 8138-8143.
39. Banjare, S. K.; Chebolu, R.; Ravikumar, P., *Organic Letters* **2019,** *21*, 4049-4053.

40. Muniraj, N.; Prabhu, K. R., *ACS omega* **2017,** *2*, 4470-4479.
41. Liu, S. L.; Li, Y.; Guo, J. R.; Yang, G. C.; Li, X. H.; Gong, J. F.; Song, M. P., *Organic Letters* **2017,** *19*, 4042-4045.
42. Li, B.; Guo, C.; Shen, N.; Zhang, X.; Fan, X., *Organic Chemistry Frontiers* **2020,** *7*, 3698-3704.
43. Schmidt, A. W.; Reddy, K. R.; Knölker, H. J., *Chemical Reviews* **2012,** *112*, 3193-3328.
44. Gu, W.; Qiao, C.; Wang, S. F.; Hao, Y.; Miao, T. T., *Bioorganic & Medicinal Chemistry Letters* **2014,** *24*, 328-331.
45. Ogawa, N.; Yamaoka, Y.; Takikawa, H.; Tsubaki, K.; Takasu, K., *The Journal of Organic Chemistry* **2018,** *83*, 7994-8002.
46. Gao, H.; Xu, Q. L.; Yousufuddin, M.; Ess, D. H.; Kürti, L., *Angewandte Chemie International Edition* **2014,** *53*, 2701-2705.
47. Parisien-Collette, S.; Cruché, C.; Abel-Snape, X.; Collins, S. K., *Green chemistry* **2017,** *19*, 4798-4803.
48. Xia, X. F.; Wang, N.; Zhang, L. L.; Song, X. R.; Liu, X. Y.; Liang, Y. M., *The Journal of Organic Chemistry* **2012,** *77*, 9163-9170.
49. Yang, X.; Li, Y.; Kong, L.; Li, X., *Organic Letters* **2018,** *20*, 1957-1960.
50. Han, Q.; Guo, X.; Tang, Z.; Su, L.; Yao, Z.; Zhang, X.; Lin, S.; Xiang, S.; Huang, Q., *Advanced Synthesis & Catalysis* **2018,** *360*, 972-984.
51. Xia, Y. Q.; Dong, L., *Organic Letters* **2017,** *19*, 2258-2261.
52. Morimoto, K.; Hirano, K.; Satoh, T.; Miura, M., *Organic Letters* **2010,** *12*, 2068-2071.
53. Ackermann, L.; Wang, L.; Lygin, A. V., *Chemical Science* **2012,** *3*, 177-180.
54. Chen, G.; Zhang, X.; Jia, R.; Li, B.; Fan, X., *Advanced Synthesis & Catalysis* **2018,** *360*, 3781-3787.
55. Li, B.; Zhang, B.; Zhang, X.; Fan, X., *Chemical Communications* **2017,** *53*, 1297-1300.
56. Liu, L.; Jiang, P.; Liu, Y.; Du, H.; Tan, J., *Organic Chemistry Frontiers* **2020,** *7*, 2278-2283.
57. Zheng, G.; Duan, X.; Chen, L.; Sun, J.; Zhai, S.; Li, X.; Jing, J.; Li, X., *The Journal of Organic Chemistry* **2020,** *85*, 4543-4552.
58. Guo, S.; Liu, Y.; Zhao, L.; Zhang, X.; Fan, X., *Organic Letters* **2019,** *21*, 6437-6441.

59. Wang, X.; Zhang, J.; Chen, D.; Wang, B.; Yang, X.; Ma, Y.; Szostak, M., *Organic Letters* **2019,** *21*, 7038-7043.
60. Liu, Y.; Yang, Z.; Chauvin, R.; Fu, W.; Yao, Z.; Wang, L.; Cui, X., *Organic Letters* **2020,** *22*, 5140-5144.
61. Deslandes, S.; Chassaing, S.; Delfourne, E., *Marine Drugs* **2009,** *7*, 754-786.
62. Lavrard, H.; Rodriguez, F.; Delfourne, E., *Bioorganic & Medicinal Chemistry* **2014,** *22*, 4961-4967.
63. Hugon, B.; Anizon, F.; Bailly, C.; Golsteyn, R. M.; Pierré, A.; Léonce, S.; Hickman, J.; Pfeiffer, B.; Prudhomme, M., *Bioorganic & Medicinal Chemistry* **2007,** *15*, 5965-5980.
64. Nakano, H.; Ōmura, S., *The Journal of Antibiotics* **2009,** *62*, 17-26.
65. Lee, S.; Kim, K. H.; Cheon, C.-H., *Organic Letters* **2017,** *19*, 2785-2788.
66. Meragelman, K. M.; West, L. M.; Northcote, P. T.; Pannell, L. K.; McKee, T. C.; Boyd, M. R., *The Journal of Organic Chemistry* **2002,** *67*, 6671-6677.
67. Qi, Z.; Yu, S.; Li, X., *The Journal of Organic Chemistry* **2015,** *80*, 3471-3479.
68. Li, P.; Zhang, X.; Fan, X., *The Journal of Organic Chemistry* **2015,** *80*, 7508-7518.
69. Hu, H.; Li, G.; Hu, W.; Liu, Y.; Wang, X.; Kan, Y.; Ji, M., *Organic Letters* **2015,** *17*, 1114-1117.
70. Qi, X.; Li, Y.; Bai, R.; Lan, Y., *Accounts of Chemical Research* **2017,** *50*, 2799-2808.
71. Ghorai, D.; Dutta, C.; Choudhury, J., *ACS Catalysis* **2016,** *6*, 709-713.
72. Kwak, J.; Ohk, Y.; Jung, Y.; Chang, S., *Journal of the American Chemical Society* **2012,** *134*, 17778-17788.
73. Butschke, B.; Schwarz, H., *Chemical Science* **2012,** *3*, 308-326.
74. Robinson, B., *Chemical Reviews* **1963,** *63*, 373-401.
75. Hughes, D. L., *Organic Preparations and Procedures International* **1993,** *25*, 607-632.
76. Wu, W. B.; Huang, J. M., *Organic Letters* **2012,** *14*, 5832-5835.
77. Dolomanov, O. V.; Bourhis, L. J.; Gildea, R. J.; Howard, J. A.; Puschmann, H., *Journal of Applied Crystallography* **2009,** *42*, 339-341.
78. Sheldrick, G. M., *Acta Crystallographica Section A: Foundations and Advances* **2015,** *71*, 3-8.
79. Sheldrick, G. M., *Acta Crystallographica Section C: Structural Chemistry* **2015,** *71*, 3-8.